

Cerebral dopamine neurotrophic factor transfection in dopamine neurons using neurotensin-polyplex nanoparticles reverses 6-hydroxydopamine-induced nigrostriatal neurodegeneration

<https://doi.org/10.4103/1673-5374.321001>

Date of submission: September 21, 2020

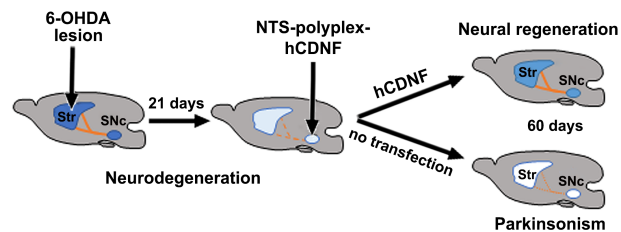
Date of decision: November 19, 2020

Date of acceptance: January 4, 2021

Date of web publication: August 30, 2021

Manuel A. Fernandez-Parrilla¹, David Reyes-Corona¹, Yazmin M. Flores-Martinez², Rasajna Nadella³, Michael J. Bannon⁴, Lourdes Escobedo¹, Minerva Maldonado-Berny¹, Jaime Santoyo-Salazar⁵, Luis O. Soto-Rojas⁶, Claudia Luna-Herrera⁷, Jose Ayala-Davila¹, Juan A. Gonzalez-Barrios⁸, Gonzalo Flores⁹, Maria E. Gutierrez-Castillo¹⁰, Armando J. Espadas-Alvarez¹⁰, Irma A. Martínez-Dávila¹, Porfirio Nava¹, Daniel Martinez-Fong^{1,11,*}

Graphical Abstract Human cerebral dopamine neurotrophic factor (hCDNF) causes neural regeneration in a Parkinson's disease model



Abstract

Overexpression of neurotrophic factors in nigral dopamine neurons is a promising approach to reverse neurodegeneration of the nigrostriatal dopamine system, a hallmark in Parkinson's disease. The human cerebral dopamine neurotrophic factor (hCDNF) has recently emerged as a strong candidate for Parkinson's disease therapy. This study shows that hCDNF expression in dopamine neurons using the neurotensin-polyplex nanoparticle system reverses 6-hydroxydopamine-induced morphological, biochemical, and behavioral alterations. Three independent electron microscopy techniques showed that the neurotensin-polyplex nanoparticles containing the hCDNF gene, ranging in size from 20 to 150 nm, enabled the expression of a secretable hCDNF *in vitro*. Their injection in the substantia nigra compacta on day 21 after the 6-hydroxydopamine lesion resulted in detectable hCDNF in dopamine neurons, whose levels remained constant throughout the study in the substantia nigra compacta and striatum. Compared with the lesioned group, tyrosine hydroxylase-positive (TH⁺) nigral cell population and TH⁺ fiber density rose in the substantia nigra compacta and striatum after hCDNF transfection. An increase in β III-tubulin and growth-associated protein 43 phospho-S41 (GAP43p) followed TH⁺ cell recovery, as well as dopamine and its catabolite levels. Partial reversal (80%) of drug-activated circling behavior and full recovery of spontaneous motor and non-motor behavior were achieved. Brain-derived neurotrophic factor recovery in dopamine neurons that also occurred suggests its participation in the neurotrophic effects. These findings support the potential of nanoparticle-mediated hCDNF gene delivery to develop a disease-modifying treatment against Parkinson's disease. The Institutional Animal Care and Use Committee of Centro de Investigación y de Estudios Avanzados approved our experimental procedures for animal use (authorization No. 162-15) on June 9, 2019.

Key Words: axonal growth; brain-derived neurotrophic factor; gene delivery; nanoparticles; neuritogenesis; neuronal cytoskeleton; neuroregeneration; neurorestoration; neurotrophic therapy; Parkinson's disease; reinnervation; substantia nigra

Chinese Library Classification No. R459.9; R364; R741

¹Departamento de Fisiología, Biofísica y Neurociencias, Centro de Investigación y de Estudios Avanzados, Ciudad de México, México; ²Programa Institucional de Biomedicina Molecular, Escuela Nacional de Medicina y Homeopatía, Instituto Politécnico Nacional, Ciudad de México, México; ³Department of Biosciences, IIIT-Srikakulam, Rajiv Gandhi University of Knowledge Technologies (RGUKT), Andhra Pradesh, India; ⁴Department of Pharmacology, Wayne State University School of Medicine, Detroit, MI, USA; ⁵Departamento de Física, Centro de Investigación y de Estudios Avanzados, Ciudad de México, México; ⁶Facultad de Estudios Superiores Iztacala, Universidad Nacional Autónoma de México, Tlalnepantla de Baz, Edo. de México, México; ⁷Departamento de Fisiología, Escuela Nacional de Ciencias Biológicas, Ciudad de México, México; ⁸Laboratorio de Medicina Genómica, Hospital Regional "1° de Octubre", ISSSTE, Ciudad de México, México; ⁹Laboratorio de Neuropsiquiatría, Instituto de Fisiología, Benemérita Universidad Autónoma de Puebla, Puebla, México; ¹⁰Departamento de Biociencias e Ingeniería, Centro Interdisciplinario de Investigaciones y Estudios sobre Medio Ambiente y Desarrollo, Instituto Politécnico Nacional, Ciudad de México, México; ¹¹Programa de Nanociencias y nanotecnología, Centro de Investigación y de Estudios Avanzados, Ciudad de México, México

*Correspondence to: Daniel Martinez-Fong, MD, PhD, martinez.fong@gmail.com.

<https://orcid.org/0000-0002-2934-8380> (Daniel Martinez-Fong)

Funding: This study was supported by the Consejo Nacional de Ciencia Tecnología (Conacyt) de México (Grant # 254686, to DMF).

How to cite this article: Fernandez-Parrilla MA, Reyes-Corona D, Flores-Martinez YM, Nadella R, Bannon MJ, Escobedo L, Maldonado-Berny M, Santoyo-Salazar J, Soto-Rojas LO, Luna-Herrera C, Ayala-Davila J, Gonzalez-Barrios JA, Flores G, Gutierrez-Castillo ME, Espadas-Alvarez AJ, Martínez-Dávila IA, Nava P, Martinez-Fong D (2022) Cerebral dopamine neurotrophic factor transfection in dopamine neurons using neurotensin-polyplex nanoparticles reverses 6-hydroxydopamine-induced nigrostriatal neurodegeneration. *Neural Regen Res* 17(4):854-866.

Introduction

Neurodegeneration and progressive loss of nigrostriatal dopamine neurons in Parkinson's disease (PD) lead to motor behavior deficits, which are the main symptom and the basis of early diagnosis (Reich and Savitt, 2019). Since the current pharmacological therapy for PD is symptomatic, different neurotrophic factor approaches have been developed to halt neurodegeneration and restore the nigrostriatal dopamine system (Nasrolahi et al., 2018). Transfection of a neurotrophic gene in dopamine neurons is an attractive approach to provide a dual neurotrophic effect on the nigrostriatal dopamine pathway through the transgenic protein released from the cell body and terminals after its anterograde axonal transport (Martinez-Fong et al., 2012).

The nanoparticle system neurotensin (NTS)-polyplex enables the targeted gene delivery via NTS receptor 1 (NTSR1) internalization to dopamine neurons *in vitro* (Hernandez-Baltazar et al., 2012) and *in vivo* (Alvarez-Maya et al., 2001). The nanoparticles result from a plasmid DNA (pDNA) compaction by the electrostatic binding of the synthetic karyophilic peptide KPRa and the conjugate of poly-L-lysine with NTS and HA2-fusogenic peptide (FP) known as NTS-carrier (Lopez-Salas et al., 2020). The peptides act sequentially to transport the pDNA toward the cell nucleus (Martinez-Fong et al., 2012). NTS binds to NTSR1 to activate the internalization of the NTS-polyplex vector (Arango-Rodriguez et al., 2006; Hernandez et al., 2014; Espadas-Alvarez et al., 2017; Aranda-Barradas et al., 2018) into nigral dopaminergic neurons that highly express NSTR1 in the plasma membrane (Martinez-Fong et al., 2012). In the endosomes, acidity activates HA2-FP to rescue the pDNA from degradation (Navarro-Quiroga et al., 2002; Arango-Rodriguez et al., 2006), and KPRa, a nuclear localization signal (NLS), transports it from the cytoplasm to the cell nucleus (Lopez-Salas et al., 2020).

NTS-polyplex nanoparticle system efficiently delivers neurotrophic factor genes even to dopamine neurons with 6-hydroxydopamine (6-OHDA) lesion (Martinez-Fong et al., 2012). The transfection of the gene coding for human glial cell-derived neurotrophic factor (hGDNF) or brain-derived neurotrophic factor (BDNF) halts the advance of nigrostriatal dopamine system neurodegeneration (Gonzalez-Barrios et al., 2006; Hernandez-Chan et al., 2015). Furthermore, the transfection of the neurturin (NRTN) gene or BDNF gene reverses nigrostriatal system neurodegeneration (Razgado-Hernandez et al., 2015; Reyes-Corona et al., 2017). NTS-polyplex nanoparticle efficacy comes from producing the transgenic neurotrophic factor in the cell body, which enables its release from both the body and axonal projection terminals after its anterograde transport (Gonzalez-Barrios et al., 2006; Hernandez-Chan et al., 2015).

Cerebral dopamine neurotrophic factor (CDNF) has shown potential for PD therapy because of its anti-neuroinflammatory, neuroprotective and neurorestorative effects on chemically induced parkinsonism (Lindholm et al., 2007) that arise from two mechanisms. The first mechanism results from its location in the lumen of the endoplasmic reticulum (ER), whose primary function is the modulation of the unfolded protein response pathway to avoid ER stress and neuroinflammation (Liu et al., 2015), as shown *in vitro* (Cheng et al., 2013; Zhao et al., 2014; Arancibia et al., 2018) and *in vivo* (Nadella et al., 2014). The second mechanism implies the release of CDNF and its binding to unidentified receptors that activate intracellular signaling pathways that finally promote neuronal restoration (Lindholm and Saarma, 2010), as shown by CDNF infusion in parkinsonian rodents and nonhuman primates (Garea-Rodriguez et al., 2016; Huttunen and Saarma, 2019).

The preventive and neurorestorative effect of CDNF has been

shown in PD models developed with 6-OHDA in rats and 1-methyl-4-phenyl-1,2,3,6-tetrahydropyridine (MPTP) in mice and nonhuman primates using several delivery approaches (Chmielarz and Saarma, 2020). Its neurorestorative effect has been demonstrated using CDNF protein delivery to the striatum through single or repeated injections or continuous infusion in rats (Voutilainen et al., 2011), mice (Airavaara et al., 2012), and nonhuman primates (Garea-Rodriguez et al., 2016), and specifically into the subventricular zone (SVZ) of rats (Nasrolahi et al., 2019). CDNF gene delivery to the striatum has also been explored using the recombinant adeno-associated virus (AAV8) (Wang et al., 2017a). Importantly, intermittent monthly bilateral intraputamenal infusions of CDNF are currently being tested in a randomized placebo-controlled phase I–II clinical study in moderately advanced PD patients (Huttunen and Saarma, 2019). Initial data suggest that CDNF is safe and shows encouraging therapeutic effects (Chmielarz and Saarma, 2020).

The neurorestorative effect of hCDNF in gene therapy has been mainly shown by dopamine phenotype recovery and motor deficit reversal (Lindholm et al., 2007; Ren et al., 2013). However, the association with neurostructural markers and hCDNF presence in projection terminals remains unknown. Here, we explored whether the association between dopaminergic neural regeneration and hCDNF presence occurs using NTS-polyplex nanoparticle-mediated hCDNF gene delivery to dopamine neurons after 21 days of a 6-OHDA lesion.

Materials and Methods

Plasmid pNBRE-hCDNF

pNBRE3x-hCDNF plasmid (4485 bp) encodes hCDNF under the transcriptional control of the synthetic NBRE3x promoter that is responsive to Nurr1 in dopamine neurons (Sacchetti et al., 2001; Espadas-Alvarez et al., 2017). This plasmid was obtained from the plasmids pCR3.1-hCDNF and pGL2-Basic-NBRE3x-luc (Nadella et al., 2014).

Synthesis of the NTS-carrier and assembly of the NTS-polyplex

The detailed procedure of NTS-carrier synthesis, a conjugate of NTS (Sigma-Aldrich, St. Louis, MO, USA) and HA2 FP (> 90% purity; Peptide 2.0; Chantilly, VA, USA) with poly-L-lysine (Sigma-Aldrich) was described previously (Arango-Rodriguez et al., 2006).

The NTS-polyplex nanoparticles were electrostatically assembled by binding the cationic NTS-carrier with the anionic KPRa-pNBRE3x-hCDNF complex (**Figure 1A**) in two steps using Dulbecco's modified Eagle's medium (DMEM; Thermo Scientific, Rockford, IL, USA) as a vehicle (Navarro-Quiroga et al., 2002; Hernandez-Baltazar et al., 2012).

First step. The KPRa-pNBRE3x-hCDNF complex is formed by incubating increasing concentrations (1–13 μ M) of cationic KPRa (KMAPKKRK; > 90% purity; Peptide 2.0; Chantilly, VA, USA) to an invariable 6 nM pNBRE3x-hCDNF (anionic). After 30-minute incubation, an electrophoretic retardation assay was performed by subjecting the samples at 80 V for 30 minutes in a 0.8% agarose gel using 40 mM Tris-Acetate, 1 mM EDTA buffer, pH8 (TAE). The gel was stained with ethidium bromide (10 μ g/mL) to select the KPRa concentration (6 μ M) that delays pNBRE3x-hCDNF band migration up to half of the control band (**Figure 1B**), based on the criterion previously established (Navarro-Quiroga et al., 2002; Hernandez-Baltazar et al., 2012). A recent report shows that at that molar ratio (6 μ M KPRa:6 nM pDNA), the KPRa-pDNA complex leaves free negative charges to allow binding of the NTS-carrier in the following step (Lopez-Salas et al., 2020).

Second step. The NTS-polyplex nanoparticles are formed by

incubating the KPRa-pNBRE3x-hCDNF complex (6 μ M KPRa: 6 nM pNBRE3x-hCDNF) with increasing concentrations (1–45 nM) of NTS-carrier. After 30 min incubation, the samples were subjected to electrophoretic retention gel assay using the conditions described above. According to the criterion previously established (Navarro-Quiroga et al., 2002; Arango-Rodriguez et al., 2006; Hernandez-Baltazar et al., 2012; Martinez-Fong et al., 2012), the optimum molar ratio was obtained at 30 nM NTS-carrier concentration, which follows the concentration producing the last visible retention of the KPRa-pNBRE3x-hCDNF band. The selected NTS-concentration produces the complete neutralization of the KPRa-pDNA complex charges (Lopez-Salas et al., 2020). The optimum molar ratio to assemble functional NTS-nanoparticles was 6 nM pNBRE3x-hCDNF:6 μ M KPRa:30 nM NTS-carrier (**Figure 1C**), the total amount of pNBRE3x-hCDNF injected into the substantia nigra pars compacta (SNc) was 260 ng (based on plasmid weight).

Electron microscopy analysis of NTS-polyplex nanoparticles

The Advanced Laboratory of Electron Nanoscopy of the Center for Research and Advanced Studies (CINVESTAV) characterized NTS-polyplex nanoparticles using field emission scanning electron microscopy (FE-SEM; Zeiss GmbH Auriga-39-16; Oberkochen, Germany) at 20 kV, transmission electron microscopy (TEM; JEM 2010, JEOL, Ltd., Tokyo, Japan) at 200 kV, and scanning probe microscope (SPM; JSPM 5200; JEOL, Ltd.) in atomic force microscopy (AFM) mode. The detailed procedures for TEM (Arango-Rodriguez et al., 2006) and FE-SEM (Espadas-Alvarez et al., 2017) were previously reported. For AFM analysis, 5 μ L of NTS-polyplex nanoparticles containing the plasmid pNBRE3x-hCDNF in DMEM was added, and a thin smear was made over a glass slide and left for few minutes, then the sample was scanned by the SPM operated in AFM contact mode. Image processing and topography analysis were done with WinSPM Data Processing System Software (Version 2.15, R. B. Leane, JEOL Ltd.).

Biological functionality of NTS-polyplex nanoparticles *in vitro*

NTS-polyplex nanoparticle-mediated transfection of pNBRE3x-hCDNF plasmid was tested in N1E-115 cells (ATCC; Manassas, VA, USA) cotransfected with pCMV-Script-Nurr1 using lipofectamine 2000 (Life Technologies, San Diego, CA, USA) to express Nurr1 (N1E-115-Nurr1 cells) and thus activating NBRE3x promoter (Espadas-Alvarez et al., 2017). After 48 hours post-transfection, hCDNF was detected through immunofluorescence in cells counterstained with 1 μ M Hoechst 33258 (Sigma-Aldrich) and quantified by enzyme-linked immunosorbent assay (ELISA), as described below.

Animals

One hundred and twenty male Wistar rats of 2-month-old (body weight 210–230 g) were obtained from the animal facilities at CINVESTAV and housed in rooms with an inverted 12-hour light/dark cycle, constant temperature ($23 \pm 2^\circ\text{C}$), and humidity ($55 \pm 5\%$). Water and food were available *ad libitum*. Animals ($n = 120$) were randomly grouped as follows: 1) The healthy untransfected group (UT; $n = 20$) evaluated on day 81 after the study initiation; 2) The initial lesion group (L21; $n = 20$) evaluated on day 21 after 6-OHDA (Sigma-Aldrich) lesion; 3) The final lesion group evaluated on day 81 after 6-OHDA injection (L81; $n = 20$); 4) Three transfection groups (T15, T30, T60; $n = 20$ per time point) that were all transfected on day 21 post-lesion (day 0) and evaluated on days 15, 30 and 60 post-transfection (**Additional Figure 1**).

All procedures were performed under the current Mexican legislation, NOM-062-ZOO-1999 (SAGARPA), based on the Guide for the Care and Use of Laboratory Animals, National Research Council. Our experimental procedures for animal use were approved by the Institutional Animal Care and Use Committee of Centro de Investigación y de Estudios Avanzados

(authorization No. 162-15; approval date: June 9, 2019). The total number of animals was 120, a minimum required by the experimental design in compliance with the Guide for the Care and Use of Laboratory Animals (The National Academies Collection: Reports funded by National Institutes of Health, 2011). Throughout the study, all efforts were made to minimize animal suffering.

Intracranial injections of 6-OHDA

Rats were anesthetized with a mixture of ketamine (120 mg/kg) and xylazine (9 mg/kg) (both anesthetics were from PISA Agropecuaria, Guadalajara, Jalisco, Mexico), injected intraperitoneally. 6-OHDA was prepared at a concentration of 20 μ g free base in 3 μ L of phosphate-buffered saline solution (PBS) containing 0.2% ascorbic acid (Sigma-Aldrich) and injected into the left striatum at the following coordinates according to the stereotaxic atlas of the rat brain (Paxinos and Watson, 1998): anteroposterior (AP), +7.7 mm from the interaural midpoint; mediolateral (ML), +4.0 mm from the intraparietal suture; dorsoventral (DV), –5.4 mm from the dura mater (Nadella et al., 2014). At 21 days post-lesion (L21), when apoptosis ended (Hernandez-Baltazar et al., 2013), 3 μ L of NTS-polyplex containing the plasmid pNBRE3x-hCDNF was injected into the lesioned SNc at a flow rate of 0.1 μ L/min. The SNc coordinates (Paxinos and Watson, 1998): AP, +2.5 mm from the interaural midpoint; ML, +2.0 mm from the intraparietal suture; DV, –6.7 mm from the dura mater (Nadella et al., 2014).

Dissection of cerebral nuclei for molecular and biochemical assays

The brain was obtained free of meninges and immediately submerged in cold PBS. Then 0.5-mm coronal slices were sectioned using a cold metallic rat brain matrix (Stoelting, Wood Dale, IL, USA) to dissect the SNc and striatum as previously reported (Flores-Martinez et al., 2018). Each sample was immediately stored in a respective Eppendorf tube at -70°C until used for ELISA, western blot, and high-performance liquid chromatography (HPLC).

ELISA

hCDNF levels were measured in pellets and culture medium of N1E-115-Nurr1 cells and SNc and striatum homogenates using ELISA type sandwich and SEG458Hu kit (Uscn Life Science Inc., Wuhan, Hubei, China), as described previously (Nadella et al., 2014). The absorbance of samples was read at 450 nm using an iMarkTM Microplate Absorbance Reader (Bio-Rad Laboratories, Hercules, CA, USA). The detection range was 15.6–1000 pg/mL. Total protein was determined using the PierceTM BCA protein assay kit (Thermo Scientific), and the values were expressed as pg/mg protein.

Western blot assay

β III-Tubulin and GAP43p were detected by western blot in 50 μ g of SNc homogenates following the procedure reported elsewhere (Hernandez-Baltazar et al., 2013). Total protein was determined using the PierceTM BCA protein assay kit (Thermo Scientific). The primary antibodies were incubated overnight at 4°C , whereas the secondary antibodies were incubated for 2 hours at room temperature. The primary antibodies were rabbit anti- β III-tubulin (1:1000; T2200; Sigma-Aldrich) and rabbit anti-growth-associated protein 43 phospho-S41 (GAP43p; 1:1:5000; Abcam; Cambridge, MA, USA). The secondary antibody was a donkey anti-rabbit IgG conjugated with horseradish peroxidase (HRP; 1:5000; Zymed, Cambridge, MA, USA). After stripping, the membranes were incubated with a mouse monoclonal antibody against glyceraldehyde 3-phosphate dehydrogenase (GA3PDH; 1:5000; AB8245; Abcam), followed by an HRP-conjugated goat anti-mouse (1:5000; Zymed). Proteins were detected using the ECL Western blotting system and Hyperfilm ECL (Amersham,

Buckinghamshire, UK). ImageJ software v.1.52h (National Institutes of Health, Bethesda, MD, USA) was used for densitometry of protein bands whose values (arbitrary units) were doubly normalized first with the densitometric values of the GAPDH band and then with the values of control without treatment.

High-performance liquid chromatography

The contents of dopamine, DOPAC (3,4-dihydroxyphenylacetic acid), and HVA (homovanillic acid) were measured in 20 μ L of homogenates of the SNc and striatum by HPLC as described previously (Reyes-Corona et al., 2017). The pellets were resuspended in 120 μ L of 0.1 M NaOH for protein determination using the Pierce™ BCA protein assay kit (Thermo Scientific). The values were expressed as pg of catecholamine/ μ g protein.

Double immunofluorescence and tyrosine hydroxylase-immunohistochemistry assays

Animals were transcardially perfused with 150 mL of cold PBS, followed by 150 mL of 4% paraformaldehyde in PBS. The brain was cut into successive coronal 30- μ m slices for the double immunofluorescence procedure described elsewhere (Nadella et al., 2014; Reyes-Corona et al., 2017). The primary antibodies were incubated overnight at 4°C, whereas the secondary antibodies were incubated for 2 hours at room temperature. The primary antibodies were rabbit polyclonal anti-CDNF (1:1000; ProSci Inc., San Diego, CA, USA), which detects both rat and human CDFN, mouse anti-tyrosine hydroxylase (TH; 1:800; MAB7566; R&D Systems, Minneapolis, MN, USA), polyclonal rabbit anti- β III-tubulin (1:300; T2200; Sigma-Aldrich), and rabbit anti-BDNF (1:500; ab108319; Abcam). An irrelevant antibody of the same IgG subclass substituted the primary antibody in all the negative controls. The secondary antibodies were Texas Red goat anti-rabbit IgG (H+L) (1:400; Vector Laboratories; Burlingame, CA, USA), Alexa Fluor 488 chicken anti-mouse IgG (H+L) (1:200; Invitrogen Molecular Probes, Eugene, OR, USA), Texas Red horse anti-mouse IgG (H+L) (1:900; Vector Laboratories), and Alexa Fluor 488 chicken anti-rabbit IgG (H+L) (1:200; Invitrogen Molecular Probes; Eugene, Oregon, USA). Fluorescence labeling was analyzed with a multispectral confocal laser-scanning microscope SP8 (TCS-SPE, Leica, Nussloch, Germany) at excitation-emission wavelengths of 405–465 nm (blue channel) for Hoechst nuclear staining, 488–522 nm (green channel) for Alexa Fluor 488, and 568–635 nm (red channel) for Texas Red. Serial 1- μ m optical sections were also obtained in the Z-series (scanning rate 600 Hz). The images were acquired using LAS AF software (Leica application suite; Leica Microsystems, Nussloch, Germany).

TH-immunohistochemistry was performed as described previously (Soto-Rojas et al., 2020c). The primary antibody was a mouse monoclonal anti-TH clone TH-2 (1:1000; Sigma-Aldrich) incubated overnight at 4°C, and the secondary antibody was a horse biotinylated anti-mouse IgG (H+L) (1:200; Vector Laboratories) incubated for 2 hours at room temperature. The immunohistochemical staining was observed with a Leica DMIRE2 microscope (Leica) through 1.6 \times , 5 \times , and 20 \times objectives, and images were digitalized with a DC300F camera (Leica) for quantification of TH⁺ bodies and terminals.

Neuron counting and ramification densitometry

ImageJ software v.1.49r (National Institutes of Health) was used to count TH⁺ neurons in the SNc and measure the total density area of TH⁺ fibers in the SNc and striatum (Soto-Rojas et al., 2020c). All background intensity was eliminated from the immunohistochemically stained area to quantify only TH⁺ immunoreactivity. Counting of TH⁺ cells and fibers was performed in five anatomical levels per nucleus of six independent rats per experimental condition. The mean

value calculated from those quantifications was the final measurement in each time evaluated ($n = 6$ for every experimental condition). The same procedure was followed to quantify immunofluorescence area density (IFAD).

Spontaneous behavior tests

Four rats randomly selected from each group were evaluated with tests that measure spontaneous behavior following the procedures described in detail elsewhere (Soto-Rojas et al., 2020a, b). Vibrissae-evoked forelimb placing test and limb-use asymmetry test assessed spontaneous motor asymmetry (Schallert and Woodlee, 2004). The former test was evaluated through unsuccessful trials of the forepaw contralateral to the lesion expressed as a percentage. The beam walking test measured bradykinesia and dysbalance. The olfactory test was used to evaluate non-motor behavior (Van Kampen et al., 2015).

Circling behavior test

Ipsilateral turning behavior activated by DL-methamphetamine (8 mg/kg body weight, i.p.; Sigma-Aldrich), dose selected from our previous reports (Galarraga et al., 1987; Floran et al., 1990; Aceves et al., 1991), was evaluated a day after the spontaneous behavior testing and recorded at 1-minute intervals over 90 minutes (Reyes-Corona et al., 2017). We selected the rats that show ≥ 1000 total ipsilateral turns to avoid spontaneous recovery from the nigrostriatal lesion.

Statistical analysis

All values were expressed as the mean \pm standard deviation (SD) obtained from a minimum of four independent rats. The comparison among the groups was made using a one-way analysis of variance followed by Bonferroni *post hoc* test using GraphPad Prism 5.0 (GraphPad Software Inc., San Diego, CA, USA). The accepted significance was $P < 0.05$.

Results

Physical features of NTS-polyplex nanoparticles encompassing the plasmid pNBRE3 \times -hCDFN

NTS-polyplex nanoparticles comprise the NTS-carrier, a conjugate of poly-L-lysine with NTS and HA2 FP using the crosslinker SPDP, and the KPRa-pNBRE3 \times -hCDFN complex (Figure 1A). The assembly of those components involved two electrostatic reactions initiated with the formation of the KPRa-pNBRE3 \times -hCDFN complex monitored by the electrophoretic retardation, followed by its compaction by the NTS-carrier into functional nanoparticles monitored by the retention gel assay. The electrophoretic retardation assay (Figure 1B) showed that the band of pNBRE3 \times -hCDFN (6 nM) undergoes gradual retardation when KPRa concentration increases, indicating gradual neutralization of pNBRE3 \times -hCDFN negative charges (Lopez-Salas et al., 2020). Based on the criterion to select the KPRa concentration that leaves free negative charges of pDNA to allow NTS-carrier binding (Lopez-Salas et al., 2020), the chosen concentration was 6 μ M (Figure 1B). The electrophoretic retention assay showed that the band of KPRa (6 μ M)-pNBRE3 \times -hCDFN (6 nM) complex is gradually retained in the gel well when NTS-carrier concentration increases (Figure 1C). We have demonstrated that the complete neutralization of pDNA negative charges by the NTS-carrier occurs at the concentration following that causing the band's disappearance (Lopez-Salas et al., 2020). Based on this criterion, the chosen concentration was 30 nM NTS-carrier (Figure 1C). Therefore, the optimum molar ratio to assemble functional NTS-nanoparticles was 6 nM pNBRE3 \times -hCDFN:6 μ M KPRa:30 nM NTS-carrier (Figure 1C). Electron microscopy analysis by FE-SEM displayed the spherical shape of NTS-polyplex nanoparticles at this optimum molar ratio, whereas TEM and AFM showed the classical toroids of polymer-based nanoparticles. The size measured by the three techniques was 20 to 150 nm (Figure 1D). These results

Research Article

support the accurate prediction of electrophoretic retardation and retention gel assays to form NTS-polyplex nanoparticles with a size that enables their internalization by the endosomal pathway (Arango-Rodriguez et al., 2006; Castillo-Rodriguez et al., 2014; Hernandez et al., 2014; Espadas-Alvarez et al., 2017; Aranda-Barradas et al., 2018).

hCDNF is released in N1E-115-Nurr1 cells

N1E115-Nurr1 cells were transfected with NTS-polyplex nanoparticles containing the plasmid pNBRE3x-hCDNF to test hCDNF expression driven by NBRE3x promoter. Transfection with lipofectamine was a control. ELISA measurements showed no hCDNF levels in untransfected cells (Figure 2A). In contrast, pNBRE3x-hCDNF transfection by NTS-polyplex nanoparticles or lipofectamine generated hCDNF in N1E115-Nurr1 cells (Figure 2A). hCDNF levels in the culture medium elicited by lipofectamine were higher than those by NTS-polyplex nanoparticle transfection (Figure 2A). However, the opposite trend was observed in cell extracts (Figure 2A). CDNF is a primarily ER lumen-located protein for bearing a KDEL-like ER retention sequence that can be secreted under cellular stress to protect neighboring cells in a paracrine fashion as MANF (Huttunen and Saarma, 2019) by a possible mechanism depending on cell surface KDEL receptors (Henderson et al., 2013). Lipofectamine-induced cellular stress (Fischer-Kierzkowska et al., 2011) could potentially explain the higher secretion of hCDNF compared with NTS-polyplex nanoparticles. While lipofectamine is highly efficient for *in vitro* transfections, it exerts a degree of cytotoxicity on cultured cells (Rahimi et al., 2018; Wang et al., 2018), especially in cotransfections as was used here (Wang et al., 2018). In contrast, NTS-polyplex nanoparticle transfection *in vitro* is limited by NTSR1 endocytosis (Espadas-Alvarez et al., 2017) but is safe in the concentration range used (Arango-Rodriguez et al., 2006).

The immunofluorescence assays also showed the absence of hCDNF immunoreactivity in untransfected cells and its presence in both cells transfected with lipofectamine or NTS-polyplex nanoparticles (Figure 2B). Altogether, these results show that the p3xNBRE-hCDNF plasmid is functional, enabling the expression of secreted hCDNF.

Dopamine neuron recovery from 6-OHDA lesion follows hCDNF gain

In agreement with previous reports (Nadella et al., 2014), double immunofluorescence assays against TH and CDNF revealed that CDNF was absent in TH⁺ cells but present in TH⁻ cells (Figure 3A and B) in both healthy and 6-OHDA lesioned SNc. However, 15 days after hCDNF gene transfection, CDNF immunoreactivity appeared in TH⁺ cells of the SNc with 21 days of 6-OHDA lesion, and its levels significantly increased from 30 to 60 days post-transfection, reaching the levels of healthy controls (Figure 3A and B). As expected, 6-OHDA caused an 84.4 ± 1.1% significant decrease in TH immunoreactivity on day 21 that remained until day 60 post-lesion (Figure 3A and C). Interestingly, the progressive recovery of TH immunoreactivity in the transfected group (Figure 3A and C) followed the time course of hCDNF levels (Figure 3A and B). This association suggests that hCDNF may promote the recovery of dopaminergic neurons, which are the source of hCDNF, as confirmed by the confocal orthogonal view (Additional Figure 2). ELISA measurements using a specific antibody did not detect hCDNF in the SNc of healthy rats and untransfected rats at 21 or 81 days of the lesion. In contrast, hCDNF levels were present in the SNc since days 15 to 60 post-transfection without a statistically significant difference (Table 1). ELISA measurements in the striatum also yielded similar results (Table 1), suggesting that hCDNF traveled from the SNc to the striatum via anterograde axonal transport.

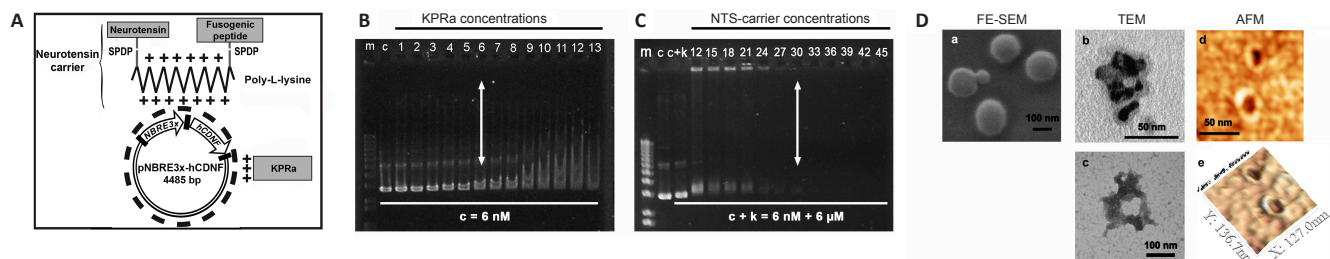
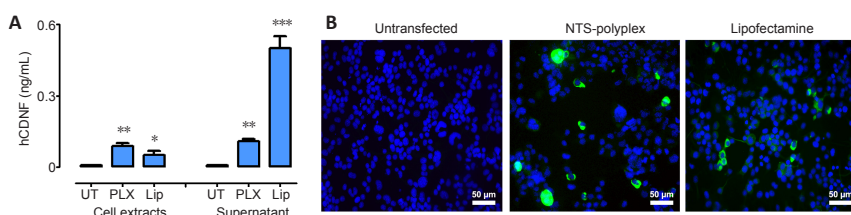


Figure 1 | Assembling of NTS-polyplex nanoparticles encompassing the plasmid pNBRE3x-hCDNF.

(A) Diagram of NTS-polyplex components. Neurotensin-carrier is the conjugate of poly-L-lysine with neurotensin and HA2 fusogenic peptide using the crosslinker SPDP. KPRa is a synthetic monomeric karyophilic peptide bound electrostatically to pNBRE3x-hCDNF, a plasmid coding for hCDNF under the control of the synthetic promoter NBRE3x. (B) Electrophoretic retardation gel assay to select the optimum molar ratio of the KPRa-pNBRE3x-hCDNF complex. Increasing KPRa concentrations (1 to 13 μM) were incubated with 6 nM pNBRE3x-hCDNF plasmid. A double arrow indicates the selected PKRa concentration (6 μM) for 6 nM pNBRE3x-hCDNF plasmid. (C) Electrophoretic retention gel assay to select the optimum molar ratio between KPRa-pNBRE3x-hCDNF complex and NTS-carrier to form functional nanoparticles. pDNA-KPRa (c+k) complex (6 nM pNBRE3x-hCDNF:6 μM KPRa) was incubated with increasing concentrations of NTS-carrier (12 to 45 nM). A double arrow indicates the selected NTS-carrier concentration (30 nM) to form functional NTS-polyplex nanoparticles. c: pDNA control; m: molecular weight markers. (D) Representative micrographs of high-resolution electron microscopy using field emission scanning electron microscopy (FE-SEM; a), transmission electron microscopy (TEM; b and c), and atomic force microscopy (AFM; d) show NTS-polyplex nanoparticles assembled at the optimum molar ratio (6 nM pNBRE3x-hCDNF: 6 μM KPRa: 30 nM NTS-carrier). Representative three-dimensional view of two individual nanoparticles taken by AFM contact mode (e). hCDNF: Human cerebral dopamine neurotrophic factor; KPRa: synthetic karyophilic peptide; NTS: nanoparticle system neurotensin; pNBRE3x: plasmid containing the synthetic NBRE3x promoter; SPDP: (succinimidyl 3-(2-pyridyl)dithio)propionate).

Figure 2 | Production and release of hCDNF in N1E115-Nurr1 cells.

(A) Soluble hCDNF was measured by enzyme-linked immunosorbent assay (ELISA) assays in conditioned media harvested from N1E115-Nurr1 cells transfected with the plasmid pNBRE3x-hCDNF using NTS-polyplex nanoparticles (PLX) or lipofectamine (Lip). Data were expressed as the mean ± SD. **P* < 0.05, ***P* < 0.01, ****P* < 0.001, vs. UT (one-way analysis of variance with Bonferroni *post hoc* test). (B) Representative micrographs from three experiments showing hCDNF immunoreactivity (green) in N1E115-Nurr1 cells with nuclear Hoechst counterstaining (blue). hCDNF: Human cerebral dopamine neurotrophic factor; NTS: nanoparticle system neurotensin; UT: untransfected.



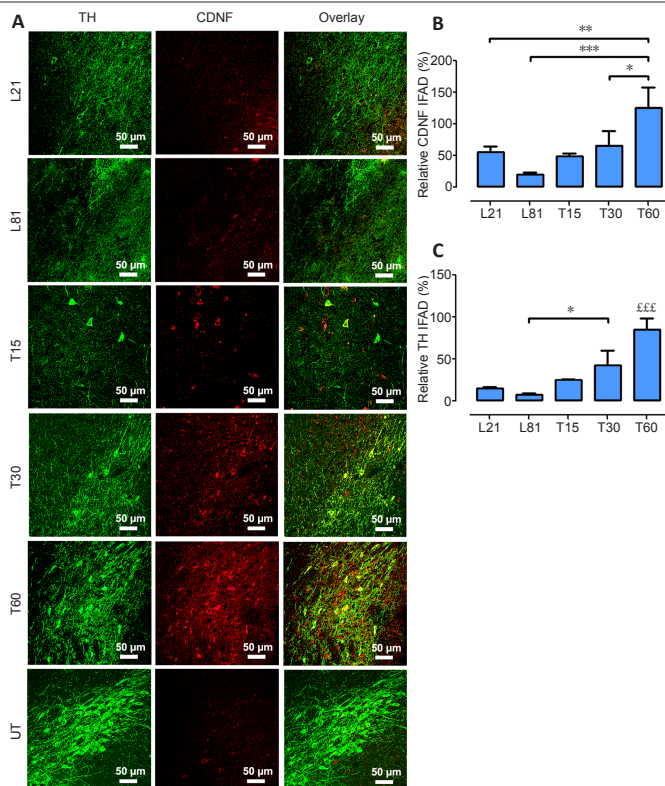


Figure 3 | Dopamine neuron recovery from the 6-OHDA lesion follows the increase in CDNF levels in the SNc.

(A) Representative confocal micrographs of CDNF-TH double immunofluorescence in the SNc of untransfected lesioned rats (L21 and L81), hCDNF-transfected and lesioned rats evaluated over time (T15, T30 and 60) and healthy control rats (UT). Scale bars: 50 μ m. (B) The immunofluorescence area density (IFAD) for CDNF (red) and (C) TH (green) was determined using ImageJ software v.1.52h. Data were expressed as the mean \pm SD ($n = 6$ independent rats each time of each experimental condition; the experiment was repeated four times) expressed relatively as a percentage of those in untransfected healthy SNc. One-way analysis of variance and Bonferroni *post hoc* test. * $P < 0.05$, ** $P < 0.01$, *** $P < 0.001$. $\text{EEEE} < 0.001$, vs. L21, L81, T15, and T30. 6-OHDA: 6-Hydroxydopamine; CDNF: cerebral dopamine neurotrophic factor; hCDNF: human CDNF; NTS: nanoparticle system neurotensin; SNc: substantia nigra pars compacta; TH: tyrosine hydroxylase.

Table 1 | hCDNF levels after CDNF gene transfection via nanoparticle system neurotensin-polyplex nanoparticles

Group	Substantia nigra	Striatum	<i>P</i>
UT	nd	nd	
L21	nd	nd	
L81	nd	nd	
T15	274.3 \pm 55.0	297.6 \pm 71.1	> 0.05
T30	353.3 \pm 67.3	324.3 \pm 42.9	> 0.05
T60	322.8 \pm 22.5	335.1 \pm 55.4	> 0.05

hCDNF levels expressed in pg/mg were measured with enzyme-linked immunosorbent assay. UT: Healthy untransfected rats. Rats with 21 days (L21) and 81 days (L81) of 6-hydroxydopamine lesion. Lesioned hCDNF-transfected rats evaluated on days 15 (T15), 30 (T30) and 60 (T60) post-transfection. CDNF: Cerebral dopamine neurotrophic factor; hCDNF: human CDNF; nd: not detected.

hCDNF gene transfection reverses the loss of dopamine neurons and striatal innervation

In the SNc, 6-OHDA decreased TH⁺ cell population by 88.7 \pm 2.8% and branching density by 84.6 \pm 9.9% (Figure 4A–C) compared with the UT group. Such a decrease remained unaltered until the end of the study, thus showing the absence of spontaneous recovery (Figure 4A and B). In contrast, hCDNF gene transfection caused a significant increase in both the number (reaching 63.1 \pm 11.2%) and branching (75.9 \pm 16.1%) of TH⁺ cells as compared with untransfected lesioned rats (Figure 4).

In the striatum, 6-OHDA decreased TH⁺ fiber density by 81.6 \pm 4.7% compared with the UT group, and the recovery was

75.1 \pm 7.6% after the intranigral hCDNF gene transfection compared with the untransfected lesioned rats (Figure 5).

In both nuclei, the recovery was progressive and significant since day 15 after transfection reaching 75.9 \pm 16.1% (SNc) and 75.1 \pm 7.6 % (striatum) of healthy condition levels at the end of the study (Figures 4 and 5).

hCDNF gene transfection recovers cytoskeleton in nigral dopamine neurons

The 6-OHDA lesion also significantly decreased the immunoreactivity of β III-tubulin, a neuronal cytoskeleton protein (Katsetos et al., 2003), in the SNc on days 21 (30%) and 60 (70%) post-lesion compared with the healthy condition (Figure 6A and B). As compared with the lesion group, hCDNF gene transfection increased β III-tubulin immunofluorescence, which was significant from day 30 post-transfection and reached 80% of the healthy condition (Figure 6A and B). Western blot results of β III-tubulin repeated the immunofluorescence pattern (Figure 6C) and also revealed a significant increase in GAP43p, a marker of axon growth and regeneration (Kawasaki et al., 2018), on days 15 and 30 post-transfection (Figure 6D). The TH immunofluorescence pattern in all the experimental groups (Figure 6A and E) was consistent with those shown in Figures 3C and 4B–C. These results suggest that hCDNF promoted dopamine neuron branching growth, consistent with the increased area density in the SNc (Figure 4A and C) and striatum (Figure 5).

Endogenous BDNF source is restored by hCDNF gene transfection

The double immunofluorescence analysis in the SNc showed that the primary source of BDNF is dopamine neurons (Figure 7A), confirming previous reports (Seroogy et al., 1994; Numan and Seroogy, 1999). Therefore, the 6-OHDA lesion decreased the number of BDNF-expressing TH⁺ cells but maintained high BDNF levels in TH[–] cells that decreased by 75% at the end of the study (L81) compared with the L21 condition (Figure 7A). Compared with the L81 condition, BDNF gain was 50% significantly higher on day 15 after hCDNF gene transfection and increased to 75% of healthy condition values on day 60 post-transfection (Figure 7A and B). At this time, most BDNF immunoreactivity was present in TH⁺ cells, whose recovery pattern was similar to those shown above (Figures 3–6). These results suggest that BDNF recovery also contributes to the hCDNF-induced reversal of nigrostriatal dopamine neurodegeneration as shown by the gradual increase in relative TH IFAD (Figure 7C).

hCDNF gene transfection increases dopamine metabolism in the SNc and striatum

6-OHDA lesion decreased dopamine levels by 75% in the SNc (Figure 8A) and by 86.5% in the striatum (Figure 8B) compared with the healthy controls. In comparison with L21 and L81 groups, a significant increase in dopamine levels occurred on days 30 and 60 after hCDNF transfection. The recovery reached 45.2 \pm 2.8% of the average healthy conditions (Figure 8A and B). However, the effect on DOPAC and HVA levels was different in each nucleus. In comparison with the healthy condition, those levels in the SNc of L21 and L81 groups were 650.32% higher, whereas the levels increased by 42.50% (DOPAC) and 68.54% (HVA) in the striatum of the same groups (Figure 8B and C). Nevertheless, DOPAC and HVA levels progressively increased in both nuclei after hCDNF transfection compared with lesion condition levels (Figure 8C and D). HVA levels in the SNc decreased at days 30 and 60 after transfection compared to the lesion groups; yet, the levels remained higher than healthy condition levels (Figure 8E). In the striatum, HVA levels decreased in the lesioned groups and recovered in the transfected groups to reach the highest values at 60 days compared with the UT values (Figure 8F). The index of the total DA catabolism rate after hCDNF transfection may indicate the scope of recovery, particularly in the striatum.

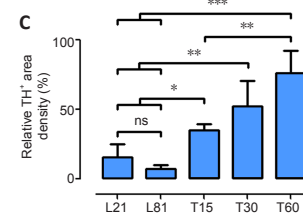
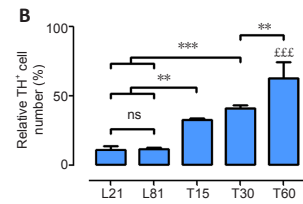
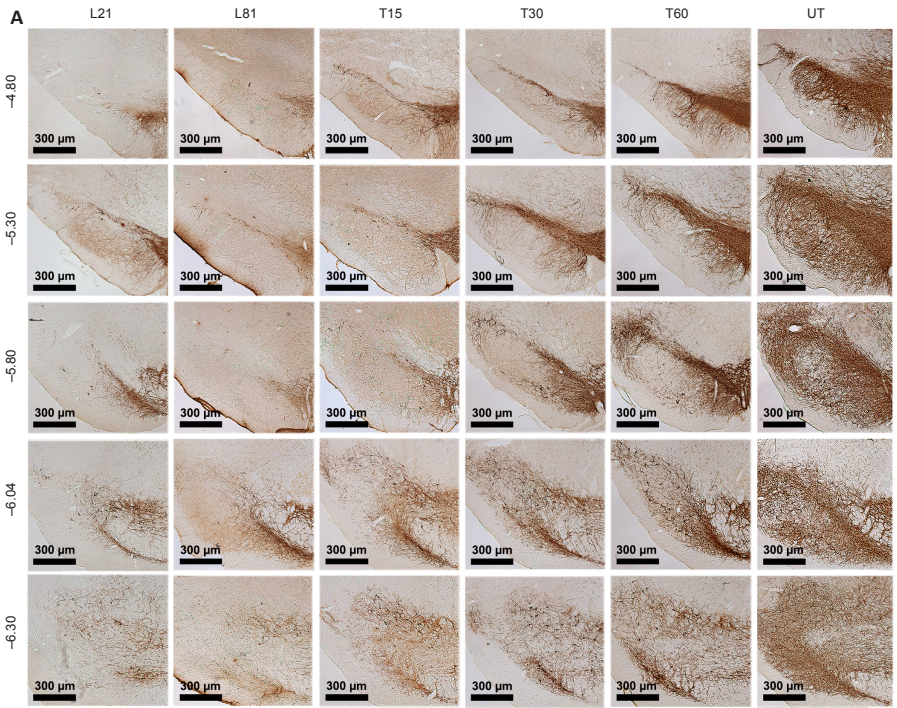


Figure 4 | hCDNF gene transfection increases TH⁺ neuron population and branching density in the SNc of rats with 6-OHDA lesion.

(A) Representative micrographs of TH immunohistochemistry. Heading shows the experimental groups. Rats with the lesion (L21 and L81) and hCDNF transfection evaluated over time (T15, T30, T60). UT: healthy untransfected rats. Anterior-posterior coordinates of Paxinos and Watson Rat Atlas appeared at left. Scale bars: 300 μm. (B, C) TH⁺ neurons (B) and TH⁺ branching area density (C) were measured with ImageJ software v.1.52h. Data are expressed as the mean ± SD (*n* = 6 independent rats each time of each experimental condition); the experiments were repeated four times expressed relatively as a percentage of those in untransfected healthy SNc. One-way analysis of variance and Bonferroni *post hoc* test. **P* < 0.05, ***P* < 0.01, ****P* < 0.001. *EEEEP* < 0.001, vs. L21, L81, T15, and T30. 6-OHDA: 6-Hydroxydopamine; CDNF: cerebral dopamine neurotrophic factor; hCDNF: human CDNF; ns: not significant; NTS: nanoparticle system neurotensin; SNc: substantia nigra pars compacta; TH: tyrosine hydroxylase.

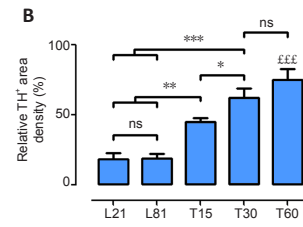
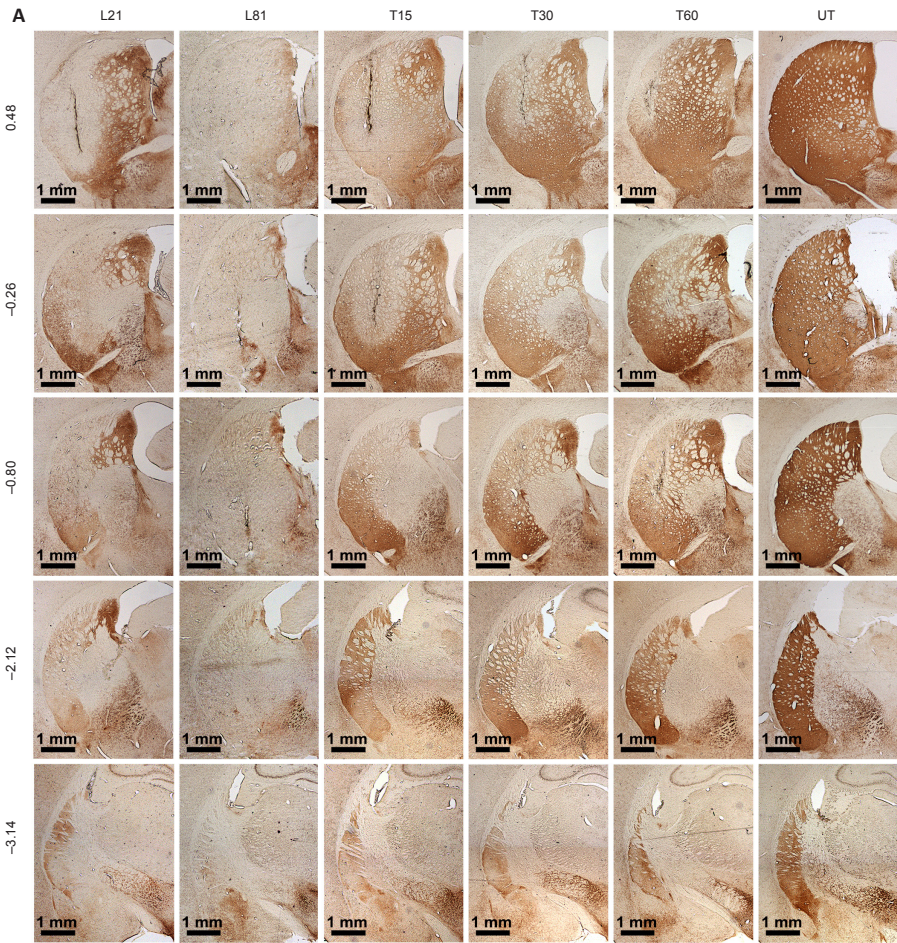


Figure 5 | hCDNF gene transfection increases TH⁺ density area in the striatum of rats with 6-OHDA lesion.

(A) Representative micrographs of TH immunohistochemistry. Heading shows the experimental groups. Rats with the lesion (L21 and L81) and transfection with hCDNF evaluated over time (T15, T30, T60). UT = healthy untransfected rats. Anterior-posterior coordinates of Paxinos and Watson Rat Atlas appeared at left. (B) TH⁺ area density was measured with ImageJ software v.1.52h. Data are expressed as the mean ± SD (*n* = 6 independent rats each time of each experimental condition); the experiments were repeated four times expressed relatively as a percentage of those in untransfected healthy striatum. One-way analysis of variance and Bonferroni *post hoc* test. **P* < 0.05, ***P* < 0.01, ****P* < 0.001. *EEEEP* < 0.001, vs. L21, L81, T15 and T30. 6-OHDA: 6-Hydroxydopamine; CDNF: cerebral dopamine neurotrophic factor; hCDNF: human CDNF; ns: not significant; TH: tyrosine hydroxylase.

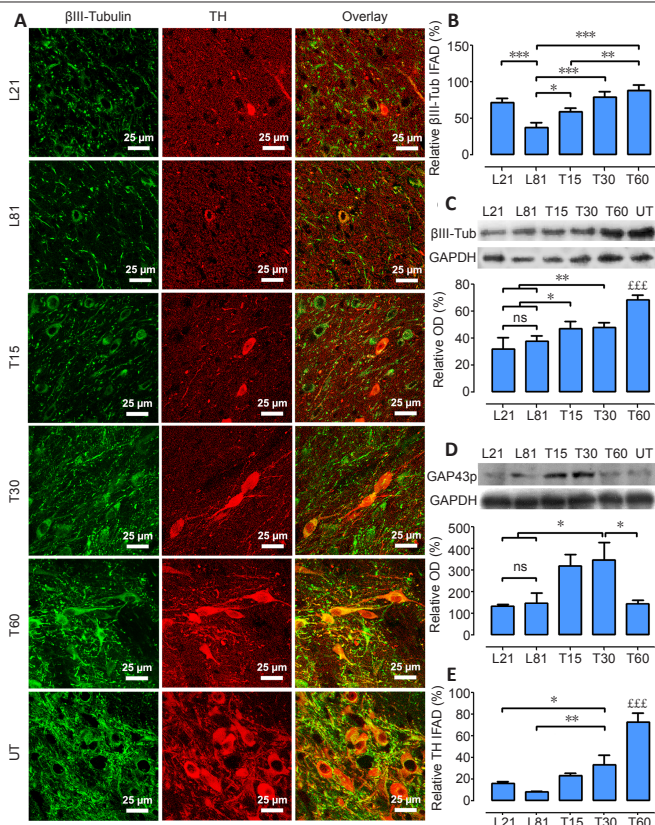


Figure 6 | hCDNF gene transfection recovers neuron cytoskeleton in TH⁺ cells of rats with 6-OHDA lesion. (A) Representative micrographs of β III-tubulin-TH double immunofluorescence in the SNc of healthy untransfected rats (UT), and rats with the lesion (L21 and L81) and transfection with hCDNF evaluated over time (T15, T30, T60). (B) Immunofluorescence area density (IFAD) for β III-tubulin (Tub). Western blot and graph of band density of β III-tubulin (C) and growth-associated protein 43 phospho-S41 (GAP43p; D). E) IFAD for TH immunoreactivity. Quantification of IFAD and band density was performed with ImageJ software v.1.52h. Data are expressed as the mean \pm SD ($n = 4$ independent rats each time of each experimental condition; the experiments were repeated four times) expressed relatively as a percentage of those in untransfected healthy SNc. One-way analysis of variance and Bonferroni *post hoc* test. * $P < 0.05$, ** $P < 0.01$, *** $P < 0.001$. $\text{£££}P < 0.001$, vs. L21, L81, T15 and T30. 6-OHDA: 6-Hydroxydopamine; CDNF: cerebral dopamine neurotrophic factor; hCDNF: human CDNF; ns: not significant; TH: tyrosine hydroxylase.

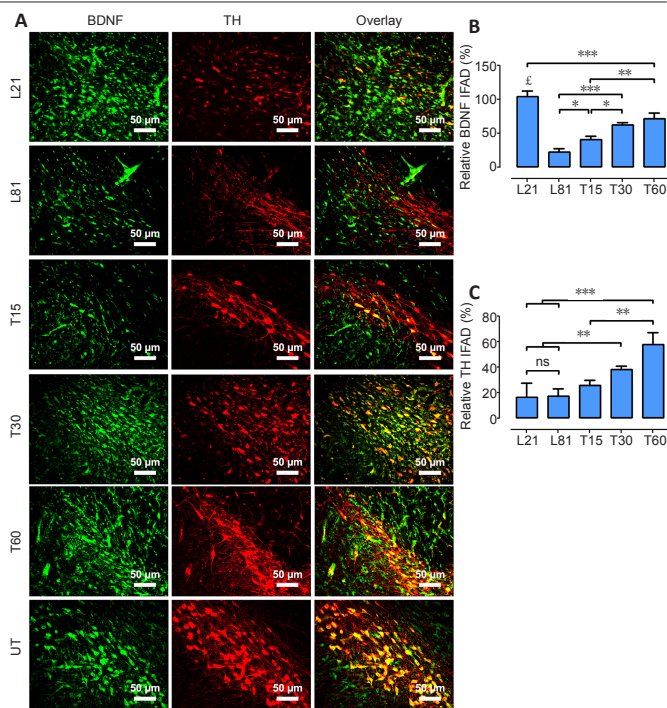


Figure 7 | hCDNF gene transfection restores BDNF levels in nigral dopamine neurons of rats with 6-OHDA lesion. (A) Representative micrographs of BDNF-TH double immunofluorescence in the SNc of control rats (UT), and rats with 6-OHDA lesion (L21 and L81) and lesioned rats with hCDNF gene transfection evaluated over time (T15, T30, T60). Immunofluorescence area density (IFAD) of BDNF (B) and TH (C) was determined using ImageJ software v.1.52h. Data are expressed as the mean \pm SD ($n = 4$ independent rats each time of each experimental condition; the experiments were repeated four times) expressed relatively as a percentage of those in untransfected healthy SNc. One-way analysis of variance and Bonferroni *post hoc* test. * $P < 0.05$, ** $P < 0.01$, *** $P < 0.001$. $\text{£P} < 0.001$, vs. L81, T15, T30 and T60. 6-OHDA: 6-Hydroxydopamine; BDNF: brain-derived neurotrophic factor; CDNF: cerebral dopamine neurotrophic factor; hCDNF: human CDNF; ns: not significant; SNc: substantia nigra pars compacta; TH: tyrosine hydroxylase.

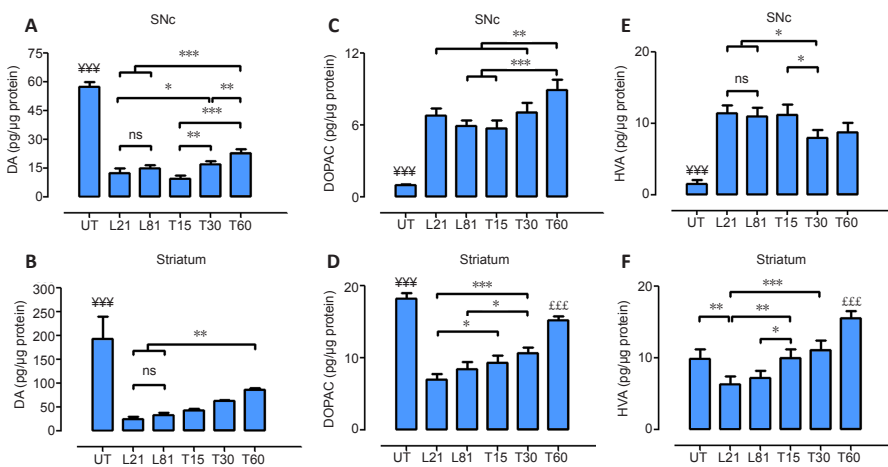


Figure 8 | hCDNF gene transfection increases dopamine and catechol levels in the SNc and striatum of rats with 6-OHDA lesion. High-performance liquid chromatography measurements were performed on days 21 and 81 after the 6-OHDA lesion (L21 and L81) and days 15, 30, 60 after hCDNF gene transfection (T15, T30, T60). (A and B) Dopamine (DA) levels. (C and D) 3,4-Dihydroxyphenylacetic acid (DOPAC) levels. (E and F) Homovanillic acid (HVA) levels. Data are expressed as the mean \pm SD ($n = 4$ independent rats each time of each experimental condition; the experiments were repeated four times). One-way analysis of variance and Bonferroni *post hoc* test. * $P < 0.05$, ** $P < 0.01$, *** $P < 0.001$. $\text{¥¥¥}P < 0.001$, vs. UT, L21, L81, T15, and T30. 6-OHDA: 6-Hydroxydopamine; CDNF: cerebral dopamine neurotrophic factor; DA: dopamine; hCDNF: human CDNF; ns: not significant; SNc: substantia nigra pars compacta.

hCDNF transfection relieves motor and non-motor behavior disability in 6-OHDA-lesioned rats
Functional recovery of the nigrostriatal dopamine system was shown through a drug-activated behavior test and four spontaneous behavior tests. The methamphetamine-activated circling behavior was 1227 ± 46.5 ipsilateral turning/90 min in the L21 group (Figure 9A) and remained unaltered in the L81 group (Figure 9A). This result shows

that the methamphetamine at the dose used here did not cause dopaminergic degeneration in the contralateral side, as confirmed by TH immunohistochemistry results in the SNc and striatum (Additional Figure 3), thus normalizing rotational behavior. hCDNF transfection significantly reduced the methamphetamine-activated circling behavior over time, although a minimum asymmetry (120 ± 41.2 ipsilateral turning/90 min) remained on day 60 after transfection (Figure

Research Article

9A). The vibrissae-evoked forelimb placing test and limb-use asymmetry test also revealed motor asymmetry in the same groups (**Figure 9B** and **C**). The disappearance of the asymmetry was complete from day 15 after hCDNF gene transfection in the vibrissae-evoked forelimb placing test (**Figure 9B**) and gradual in the limb-use asymmetry test (**Figure 9C**). The beam test revealed similar values of akinesia (**Figure 9E**) and motor discoordination (errors per step) in L21 and L81 groups (**Figure 9F**) that were gradually reduced by the hCDNF gene transfection until reaching healthy condition values (**Figure 9F**). The olfactory test showed that the rats with the lesion (L21 and L81) presented a $24.8 \pm 6.4\%$ reduction in the time of permanence in the vanilla location (olfactory stimulus) when compared with the intact rats. In contrast, lesioned and transfected rats stayed longer in the vanilla location, reaching no statistical difference to healthy rats (**Figure 9D**).

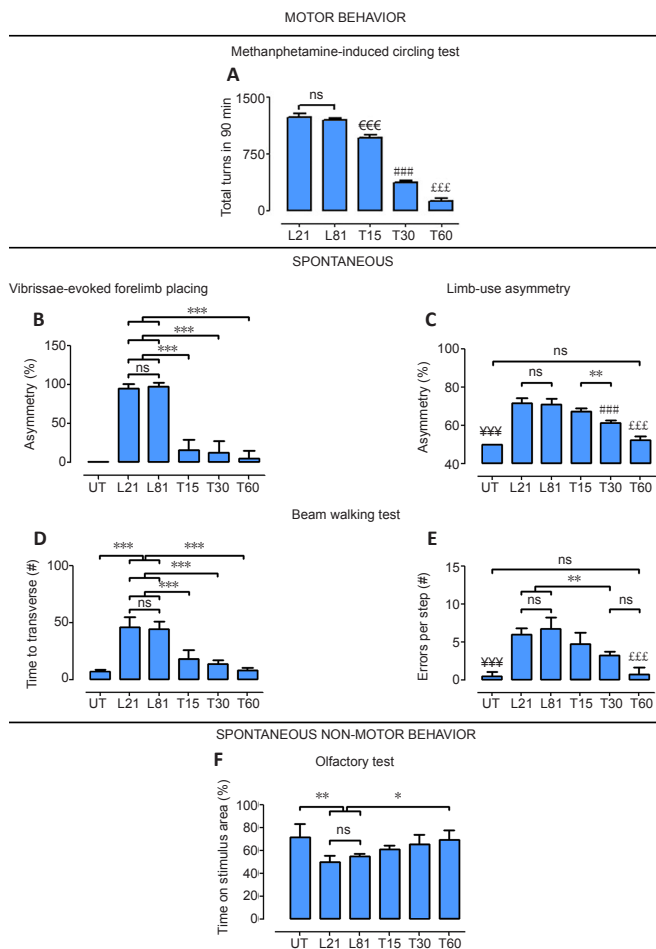


Figure 9 | Effect of CDNF gene transfection on the motor and non-motor behavior of rats with 6-OHDA lesion.

Rats were evaluated on days 21 and 81 after the 6-OHDA lesion (L21 and L81) and on days 15, 30, 60 after hCDNF gene transfection (T15, T30, T60). Data are expressed as the mean \pm SD ($n = 4$ independent rats for each time of each experimental condition; the experiments were repeated four times). One-way analysis of variance and Bonferroni *post hoc* test. * $P < 0.05$, ** $P < 0.01$, *** $P < 0.001$. €€€ $P < 0.001$, vs. UT, L21, L81, T15 and T30; ### $P < 0.001$, vs. UT, L21, L81, T15 and T60; ¥¥¥ $P < 0.001$, vs. UT, L21, L81, T30 and T60; 6-OHDA: 6-Hydroxydopamine; CDNF: cerebral dopamine neurotrophic factor; hCDNF: human CDNF; ns: not significant.

Discussion

This work shows that hCDNF transfection in dopamine neurons surviving 6-OHDA lesion can provide a secretable hCDNF (shown *in vitro*) to both nigral cells and striatal terminals, thus promoting the restoration of the nigrostriatal system. The progressive rise of β III-tubulin and GAP43p, two well-known markers of axon growth and regeneration

(Katsetos et al., 2003; Kawasaki et al., 2018), suggests that hCDNF can also stimulate neuritegenesis. This suggestion is supported by the progressive sprouting of TH⁺ nigral branches and striatal terminals following hCDNF transfection. In addition to the structural effect, hCDNF also stimulates the recovery of dopamine levels in the SNc and striatum that can account for the relief of motor and non-motor deficits. Remarkably, hCDNF transfection also increased endogenous BDNF levels in dopamine neurons with a similar time course to their restoration. This result suggests that BDNF could also mediate the hCDNF neurotrophic effect because BDNF is known to promote the survival and restoration of the nigrostriatal system in the 6-OHDA rat model (Hernandez-Chan et al., 2015; Razgado-Hernandez et al., 2015).

The progressive cell death and neuronal cytoskeleton loss caused by the intrastriatal injection of 6-OHDA in the rat reach a maximum by 21 days post-lesion, remaining 20% of surviving dopamine cells permanently (Hernandez-Baltazar et al., 2013). Because hCDNF transfection was performed at that time, then the recovery of the nigral TH⁺ cells and striatal projections confirms the restorative hCDNF effect on phenotypic markers previously reported after AAV8-mediated intrastriatal gene delivery (Wang et al., 2017a) or hCDNF intracerebral infusion in 6-OHDA lesioned rodents (Lindholm et al., 2007; Voutilainen et al., 2011, 2017; Airavaara et al., 2012) or marmoset monkeys (Garea-Rodriguez et al., 2016). Neurogenesis likely participates in dopamine cell population recovery because CDNF stimulates the proliferation and migration of neural progenitor cells of the subventricular zone in 6-OHDA-lesioned rats (Nasrolahi et al., 2019). This recovered neuronal fraction might take up the hCDNF released by the transfected neurons, thus explaining the increase in hCDNF between T15 and T30, given that the transfection was performed with a fixed amount of a plasmid. A similar phenomenon occurs with hGDNF, NRTN, and BDNF transfections (Gonzalez-Barrios et al., 2006; Razgado-Hernandez et al., 2015; Reyes-Corona et al., 2017). The CDNF uptake mechanism is still unknown; CDNF receptor-mediated endocytosis might participate, although a CDNF receptor has not yet been identified.

Moreover, the recovery of β III-tubulin and TH⁺ cells indicates that hCDNF transfection also restored the neuronal cytoskeleton of dopamine cells. The time course of the increased levels of GAP43p, a marker of axon growth and regeneration (Kawasaki et al., 2018), suggests that the more intense growth of neuronal cytoskeleton occurred in the first month after hCDNF transfection in this 6-OHDA lesion model. All these findings support that the hCDNF stimulates the regeneration of the nigrostriatal dopamine system in the 6-OHDA lesion model. Neuroprotective and neurorestorative effects of CDNF in other neurodegeneration models are also reported. Examples are contusion spinal cord injury (Zhao et al., 2016) and cerebral ischemia by middle cerebral artery occlusion (Matlik et al., 2014; Zhang et al., 2018; Anttila et al., 2019) in rats, as well as APP/PS1 model of Alzheimer's disease (Kemppainen et al., 2015) and genetic models of amyotrophic lateral sclerosis in mice (Moreno-Igoa et al., 2012).

BDNF can also mediate the neurorestorative effect of hCDNF, as supported by the association of BDNF recovery with both hCDNF expression and restoration of dopamine neurons found here. BDNF is the endogenous neurotrophic source for dopamine neurons that influences them via autocrine and paracrine mechanisms through its high-affinity receptor TrkB (Seroogy et al., 1994; Numan and Seroogy, 1999). The reduction of BDNF levels in the SNc may, therefore, contribute to the profound death of dopamine neurons induced by 6-OHDA in the rat. In contrast, the regeneration of the nigrostriatal dopamine system entails BDNF recovery, as shown here and by findings in 6-OHDA lesioned rats transfected with the BDNF gene using NTS-polyplex nanoparticles (Hernandez-Chan et al., 2015; Razgado-Hernandez et al., 2015). We

found that BDNF levels remained high on day 21 post-lesion localized to non-dopamine cells and significantly decreased (80%) on day 81 post-lesion when dopamine cell loss was maximum (80%). Glial cells are thought to be a primary BDNF source (Hisaoka-Nakashima et al., 2016) on untransfected SNc with 21 days of 6-OHDA lesion. Ongoing experiments are conducted to clarify this issue and understand the lack of neurotrophic effect. These results suggest that BDNF should be recovered in dopamine neurons to exert neurotrophic effect by an autocrine and paracrine fashion on cell bodies and projection terminals after its anterograde transport (Venero et al., 2000; Gustafsson et al., 2003).

Preclinical gene therapy studies have shown that dopamine recovery in the nigrostriatal system is essential to reverse motor disabilities (Gonzalez-Barrios et al., 2006; Hernandez-Chan et al., 2015; Razgado-Hernandez et al., 2015; Reyes-Corona et al., 2017). HPLC measurements showed that hCDNF transfection increased dopamine and its main catabolites (DOPAC and HVA) levels in the SNc and striatum, suggesting dopamine utilization. Accordingly, the altered gait, motor discoordination, and motor asymmetry were utterly eliminated in rats transfected with hCDNF, but not entirely in methamphetamine-activated circling behavior. This result suggests that postsynaptic dopamine receptor hypersensitivity remains because a complete recovery of the nigrostriatal dopamine system was not achieved at the end of the study. The possibility that the methamphetamine dose used here (8 mg of racemic mixture = 4 mg of D active enantiomer) might cause dopamine neurodegeneration in the contralateral side and normalize rotational behavior is ruled out because such a dose is in the previously reported safe range (1 to 5 mg active enantiomer) (Björklund and Dunnett, 2019). This contention is supported by preserving TH⁺ cells in nigral neurons and striatal terminals, the permanence of rotational behavior defects in the untransfected lesioned rats (L81), and the complete recovery of the spontaneous behaviors in the hCDNF transfected parkinsonian rats. Besides, the dose was acutely applied in a one-month intertrial in contrast to the neurotoxic dose that is acutely administered in three injections of 5 or 10 mg/kg at 3 or 4 hours of intervals (Wang et al., 2017b) or as a single 30 mg/kg injection (Ares-Santos et al., 2014; Yu et al., 2015). Our results are also consistent with the finding that hyposmia in 6-OHDA lesioned rats results from the loss of dopamine projections to the olfactory bulb from neurons in the SNc (Hoglinger et al., 2015). Therefore, olfaction improvement in hCDNF transfected rats indicates the reestablishment of nigro-olfactory projection following the recovery of the dopamine neuron population in the SNc. Similarly, the hCDNF-induced neural regeneration can also occur in other nuclei innervated by the nigrostriatal dopamine system.

Dopaminergic neural regeneration can be achieved with three CDNF delivery methods in parkinsonian rodents, namely direct protein injection or infusion or gene delivery. In short-term studies on acute parkinsonism (1–2 weeks of the lesion), a single CDNF (10 µg) injection in the striatum or SVZ causes neural regeneration one week after administration (Airavaara et al., 2012) and proliferation and migration of progenitor cells three weeks after treatment (Nasrolahi et al., 2019). In long-term studies in acute or chronic parkinsonian rats, repeated injections or chronic infusion of CDNF protein in rats (Voutilainen et al., 2011) and marmoset monkeys (Garea-Rodriguez et al., 2016) is needed to induce a significant neurorestoration (Voutilainen et al., 2011). In chronic parkinsonism in the rat, a single CDNF administration requires combined deep brain stimulation (Huotarinen et al., 2018) or GDNF coadministration (Voutilainen et al., 2017) to decrease neurological deficits. These studies collectively point out that the continuous presence of CDNF is needed to produce

sustained neuroregeneration of the dopaminergic nigrostriatal system. AAV8-mediated intrastriatal delivery of hCDNF gene produces sustained hCDNF production in chronic parkinsonian rats but requires the combined expression of aromatic amino acid decarboxylase gene to improve the recovery of motor function (Wang et al., 2017a). The decreased effectiveness of the intrastriatal CDNF delivery in chronic parkinsonism could be caused by its insufficient retrograde transportation by the scarce striatal terminals to cell bodies to elicit a maximal therapeutic response, as proposed for NRTN (Bartus et al., 2014). In contrast, CDNF overexpression in dopamine neurons can potentially affect the cell body and terminals after its anterograde axonal transport (Martinez-Fong et al., 2012).

The specificity of NTS-polyplex nanoparticles for dopamine neurons (Martinez-Fong et al., 1999; Alvarez-Maya et al., 2001; Navarro-Quiroga et al., 2002; Arango-Rodriguez et al., 2006; Hernandez-Baltazar et al., 2012) can account for hCDNF expression in the cell body and its distribution to the striatum, as shown previously with other transgenes in the 6-OHDA lesion model (Gonzalez-Barrios et al., 2006; Reyes-Corona et al., 2017). Their transfection efficiency yielded hCDNF levels in the range of those produced by AAV serotype 2 transduction in the 6-OHDA model (Back et al., 2013). These advantages result from proper compaction of NTS-polyplex components into functional nanoparticles shown by FE-SEM, TEM, and AFM. These results confirm the biophysical properties characterized by transmission and scanning electron microscopy, dynamic light scattering, and circular dichroism (Arango-Rodriguez et al., 2006; Castillo-Rodriguez et al., 2014; Hernandez et al., 2014; Espadas-Alvarez et al., 2017; Aranda-Barradas et al., 2018) used for a clinical formulation (Aranda-Barradas et al., 2018). The safety of NTS-polyplex nanoparticles (Hernandez et al., 2014) is another advantage that supports their clinical use.

Despite the success of NTS-polyplex nanoparticles-mediated hCDNF gene delivery in reversing 6-OHDA-induced parkinsonism, limitations regarding the animal model, administration route, and transgene regulation should be considered. The 6-OHDA model is the most frequently used but does not develop some pathological hallmarks in PD, such as α -synucleinopathy and neurotoxic A1 reactive astrocytes. NTS-polyplex nanoparticles-mediated hCDNF gene delivery should also be tested in the stereotaxic neurotoxin β -sitosterol β -d-glucoside (BSSG) model, known to develop spreading α -synucleinopathy and induction of neurotoxic A1 reactive astrocytes (Luna-Herrera et al., 2020; Soto-Rojas et al., 2020). Since NTS-polyplex nanoparticles do not cross the brain-blood barrier (BBB), their administration is via an intracranial injection in the SNc. A less invasive procedure such as focused ultrasound could be implemented to open BBB transiently and allow the intravenous administration (Xhima et al., 2018). Last, the present study lacks a long-term assessment of hCDNF expression beyond 60 days post-transfection. Since the Nurr1 dependent NBRE3 \times promoter was used to drive hCDNF expression, the hCDNF production could be insufficient or absent in severe parkinsonism, known to reduce Nurr1 expression in dopaminergic neurons (Decressac et al., 2013).

In conclusion, our results showed that hCDNF expression in dopamine neurons is a viable strategy to provide nigral neurons and striatal projection terminals with hCDNF, which reverses the nigrostriatal dopamine system neurodegeneration and motor and non-motor deficits. Additionally, the concomitant BDNF recovery can be expected to potentiate hCDNF neurotrophic effects. This approach can be used to develop a modifying-disease treatment for PD. The NTS-polyplex-mediated hCDNF gene transfection in dopamine neurons provides hCDNF to cell bodies and terminals and reverses the neurodegeneration of the nigrostriatal dopamine system.

Research Article

Acknowledgments: The authors deeply thank Dr. Mart Saarma, Institute of Biotechnology, University of Helsinki, for providing the plasmid pCR3.1-hCDNF. The authors also thank the Unit for Production and Experimentation of Laboratory Animals (UPEAL) of Cinvestav, especially Rafael Leyva, BSc, Ricardo Gaxiola, BSc, and Mr. René Pánfilo Morales for animal handling.

Author contributions: MAFP performed immunostaining experiments, stereotaxic surgeries, HPLC assays, analyzed the data, made substantial contributions to the experimental design and manuscript writing. DRC, LOSR, and CLH participated in most immunofluorescence experiments and processed, analyzed, and interpreted the results. YMFM performed and analyzed ELISA and WB experiments. RN and MMB quantified dopamine and catabolites levels by HPLC, RN also performed assays in vitro and participated in electron microscopy characterization directed by JSS. MJB provided NBRE3x sequence, and LE designed and cloned pNBRE3x-hCDNF plasmid (4482 bp). JAD undertook the behavioral tests. JAGB supervised expression assays and statistical analysis, and PN performed and analyzed GAP43p WB experiments. GF, MEGC, AJEA, IAMD, and DMF participated in the intellectual content, conception, and design of the study, and edited the manuscript and figures. DMF also provided funding, supervised experiments and data analysis, and wrote the paper. All authors have contributed to writing and editing the manuscript and approved its final version.

Conflicts of interest: The authors declare no conflicts of interest.

Financial support: This study was supported by the Consejo Nacional de Ciencia Tecnología (Conacyt) de México (Grant # 254686, to DMF).

Institutional review board statement: The experimental procedures for animal use were approved by the Institutional Animal Care and Use Committee of Centro de Investigación y de Estudios Avanzados (authorization No. 162-15) on June 9, 2019.

Copyright license agreement: The Copyright License Agreement has been signed by all authors before publication.

Data sharing statement: Datasets analyzed during the current study are available from the corresponding author on reasonable request.

Plagiarism check: Checked twice by iThenticate.

Peer review: Externally peer reviewed.

Open access statement: This is an open access journal, and articles are distributed under the terms of the Creative Commons Attribution-NonCommercial-ShareAlike 4.0 License, which allows others to remix, tweak, and build upon the work non-commercially, as long as appropriate credit is given and the new creations are licensed under the identical terms.

Additional files:

Additional Figure 1: Experimental design.

Additional Figure 2: Location of CDNF (red immunofluorescence) in nigral dopamine neurons (green immunofluorescence).

Additional Figure 3: Methamphetamine did not cause dopaminergic degeneration in the contralateral side of the substantia nigra and striatum.

References

- Aceves J, Floran B, Martinez-Fong D, Sierra A, Hernandez S, Mariscal S (1991) L-dopa stimulates the release of [3H]gamma-aminobutyric acid in the basal ganglia of 6-hydroxydopamine lesioned rats. *Neurosci Lett* 121:223-226.
- Airavaara M, Harvey BK, Voutilainen MH, Shen H, Chou J, Lindholm P, Lindahl M, Tuominen RK, Saarma M, Hoffer B, Wang Y (2012) CDNF protects the nigrostriatal dopamine system and promotes recovery after MPTP treatment in mice. *Cell Transplant* 21:1213-1223.
- Alvarez-Maya I, Navarro-Quiroga I, Meraz-Rios MA, Aceves J, Martinez-Fong D (2001) In vivo gene transfer to dopamine neurons of rat substantia nigra via the high-affinity neurotensin receptor. *Mol Med* 7:186-192.
- Anttila JE, Pöyhönen S, Airavaara M (2019) Secondary pathology of the thalamus after focal cortical stroke in rats is not associated with thermal or mechanical hypersensitivity and is not alleviated by intra-thalamic post-stroke delivery of recombinant CDNF or MANF. *Cell Transplant* 28:425-438.
- Arancibia D, Zamorano P, Andres ME (2018) CDNF induces the adaptive unfolded protein response and attenuates endoplasmic reticulum stress-induced cell death. *Biochim Biophys Acta Mol Cell Res* 1865:1579-1589.
- Aranda-Barradas ME, Márquez M, Quintanar L, Santoyo-Salazar J, Espadas-Álvarez AJ, Martínez-Fong D, García-García E (2018) Development of a parenteral formulation of NTS-polyplex nanoparticles for clinical purpose. *Pharmaceutics* 10:5.
- Arango-Rodriguez ML, Navarro-Quiroga I, Gonzalez-Barrios JA, Martinez-Arguelles DB, Bannon MJ, Kouri J, Forgez P, Rostene W, Garcia-Villegas R, Jimenez I, Martinez-Fong D (2006) Biophysical characteristics of neurotensin polyplex for in vitro and in vivo gene transfection. *Biochim Biophys Acta* 1760:1009-1020.
- Ares-Santos S, Granado N, Espadas I, Martinez-Murillo R, Moratalla R (2014) Methamphetamine causes degeneration of dopamine cell bodies and terminals of the nigrostriatal pathway evidenced by silver staining. *Neuropsychopharmacology* 39:1066-1080.
- Back S, Peranen J, Galli E, Pulkila P, Lonka-Nevalaita L, Tamminen T, Voutilainen MH, Raasmaja A, Saarma M, Mannisto PT, Tuominen RK (2013) Gene therapy with AAV2-CDNF provides functional benefits in a rat model of Parkinson's disease. *Brain Behav* 3:75-88.
- Bartus RT, Weinberg MS, Samulski RJ (2014) Parkinson's disease gene therapy: success by design meets failure by efficacy. *Mol Ther* 22:487-497.
- Björklund A, Dunnett SB (2019) The amphetamine induced rotation test: a re-assessment of its use as a tool to monitor motor impairment and functional recovery in rodent models of Parkinson's disease. *J Parkinsons Dis* 9:17-29.
- Castillo-Rodriguez RA, Arango-Rodriguez ML, Escobedo L, Hernandez-Baltazar D, Gompel A, Forgez P, Martinez-Fong D (2014) Suicide HSVtk gene delivery by neurotensin-polyplex nanoparticles via the bloodstream and GCV Treatment specifically inhibit the growth of human MDA-MB-231 triple negative breast cancer tumors xenografted in athymic mice. *PLoS One* 9:e97151.
- Cheng L, Zhao H, Zhang W, Liu B, Liu Y, Guo Y, Nie L (2013) Overexpression of conserved dopamine neurotrophic factor (CDNF) in astrocytes alleviates endoplasmic reticulum stress-induced cell damage and inflammatory cytokine secretion. *Biochem Biophys Res Commun* 435:34-39.
- Chmielarz P, Saarma M (2020) Neurotrophic factors for disease-modifying treatments of Parkinson's disease: gaps between basic science and clinical studies. *Pharmacol Rep* 72:1195-1217.
- Decressac M, Volakakis N, Björklund A, Perlmann T (2013) NURR1 in Parkinson disease--from pathogenesis to therapeutic potential. *Nat Rev Neurol* 9:629-636.
- Espadas-Alvarez AJ, Bannon MJ, Orozco-Barrios CE, Escobedo-Sanchez L, Ayala-Davila J, Reyes-Corona D, Soto-Rodriguez G, Escamilla-Rivera V, De Vizcaya-Ruiz A, Eugenia Gutierrez-Castillo M, Padilla-Viveros A, Martinez-Fong D (2017) Regulation of human GDNF gene expression in nigral dopaminergic neurons using a new doxycycline-regulated NTS-polyplex nanoparticle system. *Nanomedicine* 13:1363-1375.
- Floran B, Aceves J, Sierra A, Martinez-Fong D (1990) Activation of D1 dopamine receptors stimulates the release of GABA in the basal ganglia of the rat. *Neurosci Lett* 116:136-140.
- Flores-Martinez YM, Fernandez-Parrilla MA, Ayala-Davila J, Reyes-Corona D, Blanco-Alvarez VM, Soto-Rojas LO, Luna-Herrera C, Gonzalez-Barrios JA, Leon-Chavez BA, Gutierrez-Castillo ME, Martinez-Davila IA, Martinez-Fong D (2018) Acute neuroinflammatory response in the substantia nigra pars compacta of rats after a local injection of lipopolysaccharide. *J Immunol Res* 2018:1838921.
- Galarraga E, Bargas J, Martinez-Fong D, Aceves J (1987) Spontaneous synaptic potentials in dopamine-denervated neostriatal neurons. *Neurosci Lett* 81:351-355.
- Garea-Rodriguez E, Eesmaa A, Lindholm P, Schlumbohm C, König J, Meller B, Krieglstein K, Helms G, Saarma M, Fuchs E (2016) Comparative analysis of the effects of neurotrophic factors CDNF and GDNF in a nonhuman primate model of Parkinson's disease. *PLoS One* 11:e0149776.

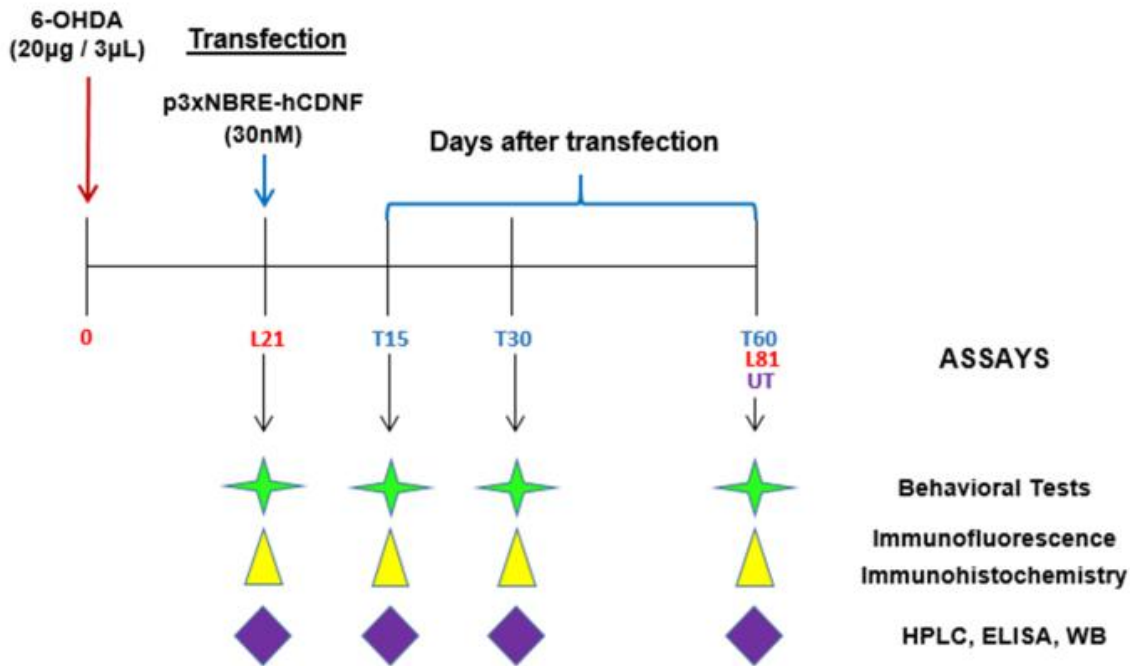
- Gonzalez-Barrios JA, Lindahl M, Bannon MJ, Anaya-Martinez V, Flores G, Navarro-Quiroga I, Trudeau LE, Aceves J, Martinez-Arguelles DB, Garcia-Villegas R, Jimenez I, Segovia J, Martinez-Fong D (2006) Neurotensin polyplex as an efficient carrier for delivering the human GDNF gene into nigral dopamine neurons of hemiparkinsonian rats. *Mol Ther* 14:857-865.
- Gustafsson E, Andsberg G, Darsalia V, Mohapel P, Mandel RJ, Kirik D, Lindvall O, Kokaia Z (2003) Anterograde delivery of brain-derived neurotrophic factor to striatum via nigral transduction of recombinant adeno-associated virus increases neuronal death but promotes neurogenic response following stroke. *Eur J Neurosci* 17:2667-2678.
- Henderson MJ, Richie CT, Airavaara M, Wang Y, Harvey BK (2013) Mesencephalic astrocyte-derived neurotrophic factor (MANF) secretion and cell surface binding are modulated by KDEL receptors. *J Biol Chem* 288:4209-4225.
- Hernandez-Baltazar D, Martinez-Fong D, Trudeau LE (2012) Optimizing NTS-polyplex as a tool for gene transfer to cultured dopamine neurons. *PLoS One* 7:e51341.
- Hernandez-Baltazar D, Mendoza-Garrido ME, Martinez-Fong D (2013) Activation of GSK-3beta and caspase-3 occurs in nigral dopamine neurons during the development of apoptosis activated by a striatal injection of 6-hydroxydopamine. *PLoS One* 8:e70951.
- Hernandez-Chan NG, Bannon MJ, Orozco-Barrios CE, Escobedo L, Zamudio S, De la Cruz F, Gongora-Alfaro JL, Armendariz-Borunda J, Reyes-Corona D, Espadas-Alvarez AJ, Flores-Martinez YM, Ayala-Davila J, Hernandez-Gutierrez ME, Pavon L, Garcia-Villegas R, Nadella R, Martinez-Fong D (2015) Neurotensin-polyplex-mediated brain-derived neurotrophic factor gene delivery into nigral dopamine neurons prevents nigrostriatal degeneration in a rat model of early Parkinson's disease. *J Biomed Sci* 22:59.
- Hernandez ME, Rembao JD, Hernandez-Baltazar D, Castillo-Rodriguez RA, Tellez-Lopez VM, Flores-Martinez YM, Orozco-Barrios CE, Rubio HA, Sanchez-Garcia A, Ayala-Davila J, Arango-Rodriguez ML, Pavon L, Mejia-Castillo T, Forgez P, Martinez-Fong D (2014) Safety of the intravenous administration of neurotensin-polyplex nanoparticles in BALB/c mice. *Nanomedicine* 10:745-754.
- Hisaoka-Nakashima K, Kajitani N, Kaneko M, Shigetou T, Kasai M, Matsumoto C, Yokoe T, Azuma H, Takebayashi M, Morioka N, Nakata Y (2016) Amitriptyline induces brain-derived neurotrophic factor (BDNF) mRNA expression through ERK-dependent modulation of multiple BDNF mRNA variants in primary cultured rat cortical astrocytes and microglia. *Brain Res* 1634:57-67.
- Hoglinger GU, Alvarez-Fischer D, Arias-Carrion O, Djufri M, Windolph A, Keber U, Borta A, Ries V, Schwarting RK, Scheller D, Oertel WH (2015) A new dopaminergic nigro-olfactory projection. *Acta Neuropathol* 130:333-348.
- Huotari A, Penttinen AM, Back S, Voutilainen MH, Julku U, Piepponen TP, Mannisto PT, Saarma M, Tuominen R, Laakso A, Airavaara M (2018) Combination of CDNF and deep brain stimulation decreases neurological deficits in late-stage model Parkinson's disease. *Neuroscience* 374:250-263.
- Huttunen HJ, Saarma M (2019) CDNF protein therapy in Parkinson's disease. *Cell Transplant* 28:349-366.
- Katsetos CD, Legido A, Perentes E, Mork SJ (2003) Class III beta-tubulin isotype: a key cytoskeletal protein at the crossroads of developmental neurobiology and tumor neuropathology. *J Child Neurol* 18:851-867.
- Kawasaki A, Okada M, Tamada A, Okuda S, Nozumi M, Ito Y, Kobayashi D, Yamasaki T, Yokoyama R, Shibata T, Nishina H, Yoshida Y, Fujii Y, Takeuchi K, Igarashi M (2018) Growth cone phosphoproteomics reveals that GAP-43 phosphorylated by JNK is a marker of axon growth and regeneration. *iScience* 4:190-203.
- Kemppainen S, Lindholm P, Galli E, Lahtinen HM, Koivisto H, Hamalainen E, Saarma M, Tanila H (2015) Cerebral dopamine neurotrophic factor improves long-term memory in APP/PS1 transgenic mice modeling Alzheimer's disease as well as in wild-type mice. *Behav Brain Res* 291:1-11.
- Lindholm P, Saarma M (2010) Novel CDNF/MANF family of neurotrophic factors. *Dev Neurobiol* 70:360-371.
- Lindholm P, Voutilainen MH, Lauren J, Peranen J, Leppanen VM, Andressoo JO, Lindahl M, Janhunen S, Kalkkinen N, Timmusk T, Tuominen RK, Saarma M (2007) Novel neurotrophic factor CDNF protects and rescues midbrain dopamine neurons in vivo. *Nature* 448:73-77.
- Liu H, Zhao C, Zhong L, Liu J, Zhang S, Cheng B, Gong L (2015) Key subdomains in the C-terminal of cerebral dopamine neurotrophic factor regulate the protein secretion. *Biochem Biophys Res Commun* 465:427-432.
- Lopez-Salas FE, Nadella R, Maldonado-Berny M, Escobedo-Sanchez ML, Fiorentino-Pérez R, Gatica-García B, Fernandez-Parrilla MA, Mario Gil M, Reyes-Corona D, García U, Orozco-Barrios CE, Gutierrez-Castillo ME, Martinez-Fong D (2020) Synthetic monopteric peptide that enables the nuclear import of genes delivered by the neurotensin-polyplex vector. *Mol Pharm* 17:4572-4588.
- Luna-Herrera C, Martinez-Davila IA, Soto-Rojas LO, Flores-Martinez YM, Fernandez-Parrilla MA, Ayala-Davila J, Leon-Chavez BA, Soto-Rodriguez G, Blanco-Alvarez VM, Lopez-Salas FE, Gutierrez-Castillo ME, Gatica-Garcia B, Padilla-Viveros A, Banuelos C, Reyes-Corona D, Espadas-Alvarez AJ, Garces-Ramirez L, Hidalgo-Alegria O, De La Cruz-Lopez F, Martinez-Fong D (2020) Intranigral administration of beta-sitosterol-beta-D-glucoside elicits neurotoxic A1 astrocyte reactivity and chronic neuroinflammation in the rat substantia nigra. *J Immunol Res* 2020:5907591.
- Martinez-Fong D, Navarro-Quiroga I, Ochoa I, Alvarez-Maya I, Meraz MA, Luna J, Arias-Montano JA (1999) Neurotensin-SPDP-poly-L-lysine conjugate: a nonviral vector for targeted gene delivery to neural cells. *Brain Res Mol Brain Res* 69:249-262.
- Martinez-Fong D, Bannon MJ, Trudeau LE, Gonzalez-Barrios JA, Arango-Rodriguez ML, Hernandez-Chan NG, Reyes-Corona D, Armendariz-Borunda J, Navarro-Quiroga I (2012) NTS-Polyplex: a potential nanocarrier for neurotrophic therapy of Parkinson's disease. *Nanomedicine* 8:1052-1069.
- Matlik K, Abo-Ramadan U, Harvey BK, Arumae U, Airavaara M (2014) AAV-mediated targeting of gene expression to the peri-infarct region in rat cortical stroke model. *J Neurosci Methods* 236:107-113.
- Moreno-Igoa M, Calvo AC, Ciriza J, Munoz MJ, Zaragoza P, Osta R (2012) Non-viral gene delivery of the GDNF, either alone or fused to the C-fragment of tetanus toxin protein, prolongs survival in a mouse ALS model. *Restor Neurol Neurosci* 30:69-80.
- Nadella R, Voutilainen MH, Saarma M, Gonzalez-Barrios JA, Leon-Chavez BA, Duenas Jimenez JM, Duenas Jimenez SH, Escobedo L, Martinez-Fong D (2014) Transient transfection of human CDNF gene reduces the 6-hydroxydopamine-induced neuroinflammation in the rat substantia nigra. *J Neuroinflammation* 11:209.
- Nasrolahi A, Mahmoudi J, Akbarzadeh A, Karimipour M, Sadigh-Eteghad S, Salehi R, Farhoudi M (2018) Neurotrophic factors hold promise for the future of Parkinson's disease treatment: is there a light at the end of the tunnel? *Rev Neurosci* 29:475-489.
- Nasrolahi A, Mahmoudi J, Karimipour M, Akbarzadeh A, Sadigh-Eteghad S, Salehi R, Farajdokht F, Farhoudi M (2019) Effect of cerebral dopamine neurotrophic factor on endogenous neural progenitor cell migration in a rat model of Parkinson's disease. *EXCLI J* 18:139-153.

Research Article

- Navarro-Quiroga I, Antonio Gonzalez-Barrios J, Barron-Moreno F, Gonzalez-Bernal V, Martinez-Arguelles DB, Martinez-Fong D (2002) Improved neurotensin-vector-mediated gene transfer by the coupling of hemagglutinin HA2 fusogenic peptide and Vp1 SV40 nuclear localization signal. *Brain Res Mol Brain Res* 105:86-97.
- Numan S, Seroogy KB (1999) Expression of trkB and trkC mRNAs by adult midbrain dopamine neurons: a double-label in situ hybridization study. *J Comp Neurol* 403:295-308.
- Paxinos G, Watson C (1998) *The rat brain in stereotaxic coordinates*, 4th ed. New York: Academic Press.
- Rahimi P, Mobarakeh VI, Kamalzare S, SajadianFard F, Vahabpour R, Zabihollahi R (2018) Comparison of transfection efficiency of polymer-based and lipid-based transfection reagents. *Bratisl Lek Listy* 119:701-705.
- Razgado-Hernandez LF, Espadas-Alvarez AJ, Reyna-Velazquez P, Sierra-Sanchez A, Anaya-Martinez V, Jimenez-Estrada I, Bannon MJ, Martinez-Fong D, Aceves-Ruiz J (2015) The transfection of BDNF to dopamine neurons potentiates the effect of dopamine D3 receptor agonist recovering the striatal innervation, dendritic spines and motor behavior in an aged rat model of Parkinson's disease. *PLoS One* 10:e0117391.
- Reich SG, Savitt JM (2019) Parkinson's disease. *Med Clin North Am* 103:337-350.
- Ren X, Zhang T, Gong X, Hu G, Ding W, Wang X (2013) AAV2-mediated striatum delivery of human CDNF prevents the deterioration of midbrain dopamine neurons in a 6-hydroxydopamine induced parkinsonian rat model. *Exp Neurol* 248:148-156.
- Reyes-Corona D, Vazquez-Hernandez N, Escobedo L, Orozco-Barrios CE, Ayala-Davila J, Moreno MG, Amaro-Lara ME, Flores-Martinez YM, Espadas-Alvarez AJ, Fernandez-Parrilla MA, Gonzalez-Barrios JA, Gutierrez-Castillo ME, Gonzalez-Burgos I, Martinez-Fong D (2017) Neurturin overexpression in dopaminergic neurons induces presynaptic and postsynaptic structural changes in rats with chronic 6-hydroxydopamine lesion. *PLoS One* 12:e0188239.
- Sacchetti P, Mitchell TR, Granneman JG, Bannon MJ (2001) Nurr1 enhances transcription of the human dopamine transporter gene through a novel mechanism. *J Neurochem* 76:1565-1572.
- Schallert T, Woodlee MT (2004) *Orienting and Placing*. In: *The behavior of the laboratory rat: a handbook with tests* (Whishaw IQ, Kolb B, eds), pp 129-140: New York: Oxford University Press.
- Seroogy KB, Lundgren KH, Tran TM, Guthrie KM, Isackson PJ, Gall CM (1994) Dopaminergic neurons in rat ventral midbrain express brain-derived neurotrophic factor and neurotrophin-3 mRNAs. *J Comp Neurol* 342:321-334.
- Soto-Rojas LO, Garces-Ramirez L, Luna-Herrera C, Flores-Martinez YM, Soto-Rodriguez G, Gatica-Garcia B, Lopez-Salas FE, Ayala-Davila J, Gutierrez-Castillo ME, Padilla-Viveros A, Banuelos C, de la Cruz-Lopez F, Martinez-Davila IA, Martinez-Fong D (2020a) A single intranigral administration of beta-sitosterol beta-d-glucoside elicits bilateral sensorimotor and non-motor alterations in the rat. *Behav Brain Res* 378:112279.
- Soto-Rojas LO, Banuelos C, Garces-Ramirez L, Luna-Herrera C, Flores-Martinez YM, Soto-Rodriguez G, Gatica-Garcia B, Lopez-Salas FE, Ayala-Davila J, Gutierrez-Castillo ME, Padilla-Viveros A, de la Cruz-Lopez F, Martinez-Davila IA, Martinez-Fong D (2020b) A sequential methodology for integral evaluation of motor and non-motor behaviors in parkinsonian rodents. *MethodsX* 7:100821.
- Soto-Rojas LO, Martinez-Davila IA, Luna-Herrera C, Gutierrez-Castillo ME, Lopez-Salas FE, Gatica-Garcia B, Soto-Rodriguez G, Bringas Tobon ME, Flores G, Padilla-Viveros A, Banuelos C, Blanco-Alvarez VM, Davila-Ayala J, Reyes-Corona D, Garces-Ramirez L, Hidalgo-Alegria O, De La Cruz-Lopez F, Martinez-Fong D (2020c) Unilateral intranigral administration of beta-sitosterol beta-D-glucoside triggers pathological alpha-synuclein spreading and bilateral nigrostriatal dopaminergic neurodegeneration in the rat. *Acta Neuropathol Commun* 8:56.
- Van Kampen JM, Baranowski DC, Robertson HA, Shaw CA, Kay DG (2015) The progressive BSSG rat model of Parkinson's: recapitulating multiple key features of the human disease. *PLoS One* 10:e0139694.
- Venero JL, Vizuete ML, Revuelta M, Vargas C, Cano J, Machado A (2000) Upregulation of BDNF mRNA and trkB mRNA in the nigrostriatal system and in the lesion site following unilateral transection of the medial forebrain bundle. *Exp Neurol* 161:38-48.
- Voutilainen MH, Back S, Peranen J, Lindholm P, Raasmaja A, Mannisto PT, Saarma M, Tuominen RK (2011) Chronic infusion of CDNF prevents 6-OHDA-induced deficits in a rat model of Parkinson's disease. *Exp Neurol* 228:99-108.
- Voutilainen MH, De Lorenzo F, Stepanova P, Bäck S, Yu LY, Lindholm P, Pörsti E, Saarma M, Männistö PT, Tuominen RK (2017) Evidence for an additive neurorestorative effect of simultaneously administered CDNF and GDNF in hemiparkinsonian rats: implications for different mechanism of action. *eNeuro* 4:ENEURO.0117-16.2017.
- Wang L, Wang Z, Zhu R, Bi J, Feng X, Liu W, Wu J, Zhang H, Wu H, Kong W, Yu B, Yu X (2017a) Therapeutic efficacy of AAV8-mediated intrastriatal delivery of human cerebral dopamine neurotrophic factor in 6-OHDA-induced parkinsonian rat models with different disease progression. *PLoS One* 12:e0179476.
- Wang L, Wang Z, Xu X, Zhu R, Bi J, Liu W, Feng X, Wu H, Zhang H, Wu J, Kong W, Yu B, Yu X (2017b) Recombinant AAV8-mediated intrastriatal gene delivery of CDNF protects rats against methamphetamine neurotoxicity. *Int J Med Sci* 14:340-347.
- Wang T, Larcher LM, Ma L, Veedu RN (2018) Systematic screening of commonly used commercial transfection reagents towards efficient transfection of single-stranded oligonucleotides. *Molecules* 23:2564.
- Xhima K, Nabbouh F, Hynynen K, Aubert I, Tandon A (2018) Noninvasive delivery of an alpha-synuclein gene silencing vector with magnetic resonance-guided focused ultrasound. *Mov Disord* 33:1567-1579.
- Yu S, Zhu L, Shen Q, Bai X, Di X (2015) Recent advances in methamphetamine neurotoxicity mechanisms and its molecular pathophysiology. *Behav Neurol* 2015:103969.
- Zhang GL, Wang LH, Liu XY, Zhang YX, Hu MY, Liu L, Fang YY, Mu Y, Zhao Y, Huang SH, Liu T, Wang XJ (2018) Cerebral dopamine neurotrophic factor (CDNF) has neuroprotective effects against cerebral ischemia that may occur through the endoplasmic reticulum stress pathway. *Int J Mol Sci* 19:1905.
- Zhao H, Cheng L, Du X, Hou Y, Liu Y, Cui Z, Nie L (2016) Transplantation of cerebral dopamine neurotrophic factor transduced BMSCs in contusion spinal cord injury of rats: promotion of nerve regeneration by alleviating neuroinflammation. *Mol Neurobiol* 53:187-199.
- Zhao H, Cheng L, Liu Y, Zhang W, Maharjan S, Cui Z, Wang X, Tang D, Nie L (2014) Mechanisms of anti-inflammatory property of conserved dopamine neurotrophic factor: inhibition of JNK signaling in lipopolysaccharide-induced microglia. *J Mol Neurosci* 52:186-192.

C-Editors: Zhao M, Liu WJ, Li CH; T-Editor: Jia Y

A Lesion



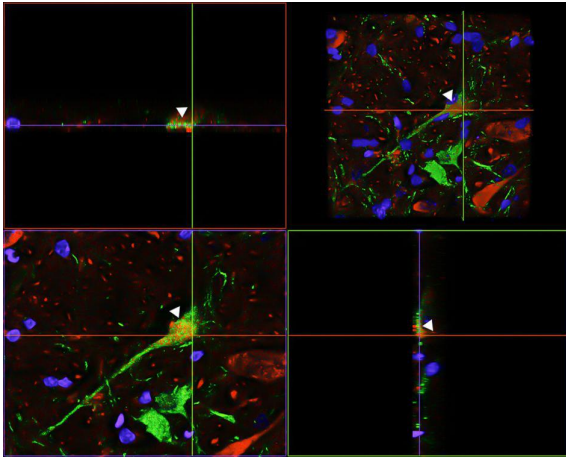
B

Number of animals:

Per group		Per experiment (X 4 repetitions)	
❖L21	n = 20	❖Immunofluorescence	n = 24
❖T15	n = 20	❖Immunohistochemistry	n = 24
❖T30	n = 20	❖ELISA	n = 24
❖T60	n = 20	❖HPLC	n = 24
❖L81	n = 20	❖WB	n = 24
❖UT	n = 20		
Total = 120		Total = 120	

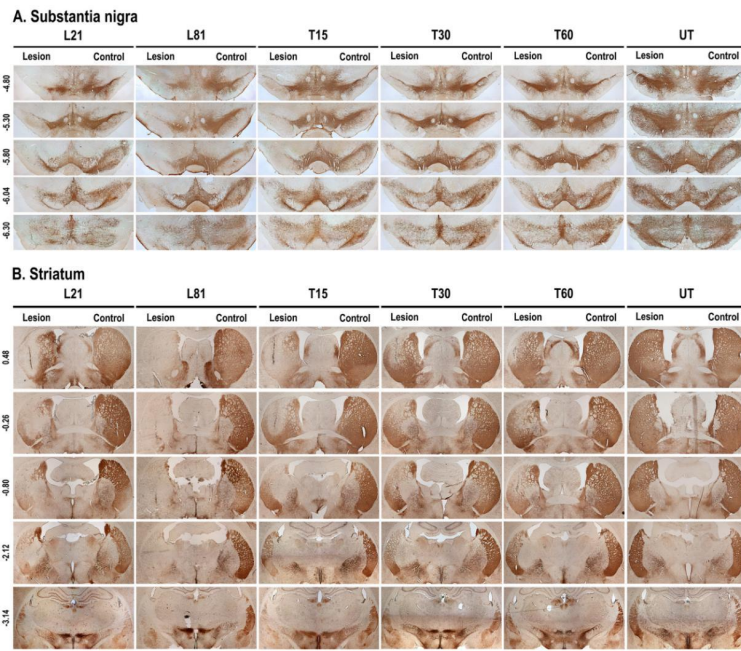
Additional Figure 1 Experimental design.

(A) Color symbols indicate when the corresponding assays were performed. (B) Table summarizes the number of animals used per assays every time point and group evaluated. Four rats of each time point were evaluated with six independent behavioral tests ($n = 4$ rats per experimental group and time). 6-OHDA: 6-hydroxydopamine; hCDNF: human cerebral dopamine neurotrophic factor; HPLC: high-performance liquid chromatography; ELISA: enzyme-linked immunosorbent assay; WB: Western Blot.



Additional Figure 2 Location of CDNF (red immunofluorescence) in nigral dopamine neurons (green immunofluorescence).

Orthogonal projections from a 1- μm z-confocal optical section are the top left and bottom right panels. The top right panel is the integrated image, and the bottom left panel is a horizontal optical Z-section. The white arrowhead indicates hCDNF (red) location in a dopamine neuron (green). Nuclear counterstaining with Hoechst (blue). The micrograph is representative of 3 independent rats with 6-hydroxydopamine lesion on day 60 after hCDNF gene transfection. hCDNF: Human CDNF; CDNF: cerebral dopamine neurotrophic factor.



Additional Figure 3 Methamphetamine did not cause dopaminergic degeneration in the contralateral side of the substantia nigra (A) and striatum (B).

Representative micrographs of TH immunohistochemistry in the cerebral hemispheres of the same rat. Heading shows the experimental groups. Rats with the lesion (L21 and L81) and hCDNF transfection evaluated over time (T15, T30, T60). UT: healthy untransfected and untreated rats. Anterior-posterior coordinates of Paxinos and Watson Rat Atlas appeared at left. hCDNF: Human cerebral dopamine neurotrophic factor.